frequently overexpressed in hepatocellular carcinoma and involved in tumor invasion. Hepatology 49:1583–1594.
53. Weng AP, Ferrando AA, Lee W, Morris JPt Silverman LB, Sanchez-Irizarry C, Blacklow SC, Look AT, Aster JC. 2004. Activating mutations of NOTCH1 in human T cell acute lymphoblastic leukemia. Science 306: 269–271.
54. Coleman ML, Sahai EA, Yeo M, Bosch M, Dewar A, Olson MF. 2001. Membrane blebbing during apoptosis results from caspase-mediated activation of ROCK I. Nat. Cell Biol. 3:339–345.
55. Sebbagh M, Renvoize C, Hamelin J, Riche N, Bertoglio J, Breard J. 2001. Caspase-3-mediated cleavage of ROCK I induces MLC phosphorylation and apoptotic membrane blebbing. Nat. Cell Biol. 3:346–352.
56. Lefort K, Mandinova A, Ostano P, Kolev V, Calpini V, Kolfschoten I, Devgan V, Lieb J, Raffoul W, Hohl D, Neel V, Garlick J, Chiorino G, Dotto GP. 2007. Notch1 is a p53 target gene involved in human keratinocyte tumor suppression through negative regulation of ROCK1/2 and MRCKalpha kinases. Genes Dev. 21:562–577.
57. Ronchini C, Capobianco AJ. 2000. Notch(ic)-ER chimeras display hormone-dependent transformation, nuclear accumulation, phosphorylation and CBF1 activation. Oncogene 19:3914–3924.
58. Krawetz RJ, Li X, Rancourt DE. 2009. Human embryonic stem cells: caught between a ROCK inhibitor and a hard place. Bioessays 31:336–343.
59. Chang J, Xie M, Shah VR, Schneider MD, Entman ML, Wei L, Schwartz RJ. 2006. Activation of Rho-associated coiled-coil protein kinase 1 (ROCK-1) by caspase-3 cleavage plays an essential role in cardiac myocyte apoptosis. Proc. Natl. Acad. Sci. U. S. A. 103:14495–14500.
60. Yatim A, Benne C, Sobhian B, Laurent-Chabalier S, Deas O, Judde JG, Lelievre JD, Levy Y, Benkirane M. 2012. NOTCH1 nuclear interactome reveals key regulators of its transcriptional activity and oncogenic function. Mol. Cell 48:445–458.
61. Yi CH, Yuan J. 2009. The Jekyll and Hyde functions of caspases. Dev. Cell 16:21–34.
62. Okuyama R, Nguyen BC, Talora C, Ogawa E, Tommasi di Vignano A, Lioumi M, Chiorino G, Tagami H, Woo M, Dotto GP. 2004. High commitment of embryonic keratinocytes to terminal differentiation through a Notch1-caspase 3 regulatory mechanism. Dev. Cell 6:551–562.
63. Lee P, Lee DJ, Chan C, Chen SW, Ch'en I, Jamora C. 2009. Dynamic expression of epidermal caspase 8 simulates a wound healing response. Nature 458:519–523.
64. Blanpain C, Fuchs E. 2009. Epidermal homeostasis: a balancing act of stem cells in the skin. Nat. Rev. Mol. Cell Biol. 10:207–217.
65. Carroll DK, Carroll JS, Leong CO, Cheng F, Brown M, Mills AA, Brugge JS, Ellisen LW. 2006. p63 regulates an adhesion programme and cell survival in epithelial cells. Nat. Cell Biol. 8:551–561.
66. Melino G. 2011. p63 is a suppressor of tumorigenesis and metastasis interacting with mutant p53. Cell Death Differ. 18:1487–1499.
67. Thumkeo D, Keel J, Ishizaki T, Hirose M, Nonomura K, Oshima H, Oshima M, Taketo MM, Narumiya S. 2003. Targeted disruption of the mouse rho-associated kinase 2 gene results in intrauterine growth retardation and fetal death. Mol. Cell. Biol. 23:5043–5055.
68. Shimizu Y, Thumkeo D, Keel J, Ishizaki T, Oshima H, Oshima M, Noda Y, Matsumura F, Taketo MM, Narumiya S. 2005. ROCK-I regulates closure of the eyelids and ventral body wall by inducing assembly of actomyosin bundles. J. Cell Biol. 168:941–953.
69. Lock FE, Hotchin NA. 2009. Distinct roles for ROCK1 and ROCK2 in the regulation of keratinocyte differentiation. PLoS One 4:e8190. doi:10.1371/journal.pone.0008190.
70. Grossi M, Hiou-Feige A, Tommasi Di Vignano A, Calautti E, Ostano P, Lee S, Chiorino G, Dotto GP. 2005. Negative control of keratinocyte differentiation by Rho/CRIK signaling coupled with up-regulation of KyoT1/2 (FHL1) expression. Proc. Natl. Acad. Sci. U. S. A. 102:11313–11318.
71. Zheng S, Huang J, Zhou K, Zhang C, Xiang Q, Tan Z, Wang T, Fu X. 2011. 17beta-Estradiol enhances breast cancer cell motility and invasion via extra-nuclear activation of actin-binding protein ezrin. PLoS One 6:e22439. doi:10.1371/journal.pone.0022439.
72. Vega FM, Fruhwirth G, Ng T, Ridley AJ. 2011. RhoA and RhoC have distinct roles in migration and invasion by acting through different targets. J. Cell Biol. 193:655–665.
73. Zhang YM, Bo J, Taffet GE, Chang J, Shi J, Reddy AK, Michael LH, Schneider MD, Entman ML, Schwartz RJ, Wei L. 2006. Targeted deletion of ROCK1 protects the heart against pressure overload by inhibiting reactive fibrosis. FASEB J. 20:916–925.
74. Lee DH, Shi J, Jeoung NH, Kim MS, Zabolotny JM, Lee SW, White MF, Wei L, Kim YB. 2009. Targeted disruption of ROCK1 causes insulin resistance in vivo. J. Biol. Chem. 284:11776–11780.

Cell Cycle 13:3, 471–481; February 1, 2014; © 2014 Landes Bioscience

ATM regulates Cdt1 stability during the unperturbed S phase to prevent re-replication

Satoko Iwahori[1], Daisuke Kohmon[2], Junya Kobayashi[3], Yuhei Tani[2], Takashi Yugawa[1], Kenshi Komatsu[3], Tohru Kiyono[1], Nozomi Sugimoto[2], and Masatoshi Fujita[2,*]

[1]Virology Division; National Cancer Center Research Institute; Chuohku, Tokyo, Japan; [2]Department of Cellular Biochemistry; Graduate School of Pharmaceutical Sciences; Kyushu University; Higashiku, Fukuoka, Japan; [3]Radiation Biology Center; Kyoto University; Sakyo-ku, Kyoto, Japan

Keywords: ATM, Cdt1, control of cell cycle progression, Akt-SCF^{Skp2}, DNA damage and repair mechanisms

Ataxia-telangiectasia mutated (ATM) plays crucial roles in DNA damage responses, especially with regard to DNA double-strand breaks (DSBs). However, it appears that ATM can be activated not only by DSB, but also by some changes in chromatin architecture, suggesting potential ATM function in cell cycle control. Here, we found that ATM is involved in timely degradation of Cdt1, a critical replication licensing factor, during the unperturbed S phase. At least in certain cell types, degradation of p27^{Kip1} was also impaired by ATM inhibition. The novel ATM function for Cdt1 regulation was dependent on its kinase activity and NBS1. Indeed, we found that ATM is moderately phosphorylated at Ser1981 during the S phase. ATM silencing induced partial reduction in levels of Skp2, a component of SCF^{Skp2} ubiquitin ligase that controls Cdt1 degradation. Furthermore, Skp2 silencing resulted in Cdt1 stabilization like ATM inhibition. In addition, as reported previously, ATM silencing partially prevented Akt phosphorylation at Ser473, indicative of its activation, and Akt inhibition led to modest stabilization of Cdt1. Therefore, the ATM-Akt-SCF^{Skp2} pathway may partly contribute to the novel ATM function. Finally, ATM inhibition rendered cells hypersensitive to induction of re-replication, indicating importance for maintenance of genome stability.

Introduction

Ataxia-telangiectasia (AT) is an autosomal recessive inherited disorder with characteristic symptoms such as cerebellar ataxia, oculocutaneous telangiectasia, and cancer predisposition. AT is caused by the mutations in the gene encoding ataxia-telangiectasia mutated (ATM) kinase, a member of the phosphoinositide 3-kinase-related protein kinase family. ATM kinase plays a pivotal role in activation of checkpoint pathways in response to DNA double-strand breaks (DSBs). When DSBs occur, ATM, together with the Mre11-RAD50-NBS1 (MRN) complex, recognizes and accumulates on lesions, where it is activated to phosphorylate many downstream effector molecules, including Chk2 kinase. Activation of the checkpoint pathway eventually leads to cell cycle arrest, repair of damage, and, under certain circumstances, apoptosis.[1-3] Indeed, cell lines derived from AT patients are hypersensitive to ionizing radiation (IR).

In addition to such classical pathways, several novel cascades regulated by ATM have recently been identified. For example, when cells are exposed to hypoxic conditions, ATM is activated and phosphorylates a transcription factor, hypoxia-inducible factor 1α, to downregulate mTORC1 signaling.[4] In this case, NBS1 is not required, and neither detectable DSB nor phosphorylation of ATM Ser1981, a marker for ATM activation, are observed. Surprisingly, ATM appears to be activated also by oxidative stress, probably through direct oxidization of ATM.[5] In addition, oxidization-induced ATM activation appears to occur in the absence of DSBs and the MRN complex. Even for the DSB-induced ATM activation, it was shown that activated ATM relocates to the cytoplasm and links DNA damage signaling to NFκB activation.[6]

The above elucidated functions of ATM protein may explain the pathogenesis of AT. However, severe and pleiotrophic symptoms in the affected patients suggest the possibility that ATM might function even in unperturbed cell cycling to maintain genome integrity. It should also be noted that molecular mechanisms underlying ATM activation upon DSB induction are still not fully understood. It has been demonstrated that ATM can be activated not only by DSB, but also by changes in chromatin architecture,[7] further suggesting potential ATM functions in unperturbed cell cycle.

From late mitosis to the G_1 phase, the sequential assembly of multiple proteins, including ORC1–6 (origin recognition complexes 1–6), Cdc6, Cdt1, and MCM2–7 (minichromosome maintenance), results in formation of a pre-replication complex (pre-RC) that is "licensed" for replication. In the late cell cycle, while the MCM helicase is activated, activity of the pre-RC components is carefully regulated so as to prohibit inappropriate

*Correspondence to: Masatoshi Fujita; Email: mfujita@phar.kyushu-u.ac.jp
Submitted: 10/29/2013; Accepted: 11/19/2013
http://dx.doi.org/10.4161/cc.27274

reassembly of pre-RC and subsequent re-replication.[8] Cdt1 strongly stimulates the licensing reaction in human cells,[9-11] and its activity is tightly restricted by multiple mechanisms during the S phase, i.e., polyubiquitination-dependent proteolysis mediated by Cdk phosphorylation-dependent SCF^{Skp2} ubiquitin ligase and the proliferating cell nuclear antigen (PCNA)-dependent Cul4-$DDB1^{Cdt2}$ ubiquitin ligase and inhibitory geminin binding.[8] Overexpression of Cdt1, ORC1, or Cdc6 alone induces no detectable re-replication in normal human cells, but co-overexpression of Cdt1 plus ORC1 or Cdc6 yields a moderate level of re-replication.[11] Cdt1 mutants deficient in S-phase degradation feature more re-replication than the wild type.[11] In certain cancer-derived cells, Cdt1 overexpression alone can induce overt re-replication.[9-11] Under such circumstances, ATM- and Rad3-related (ATR) kinase, a close relative of ATM, and the MRN complex inhibit further re-replication.[12] All of these findings clearly show that degradation of Cdt1 during S phase is critical for maintenance of genomic stability. Actually, deregulation of Cdt1 is harmful to genomic stability.[13]

Here, we sought to clarify potential novel ATM functions during the unperturbed cell cycle and found that ATM is required for proper degradation of Cdt1 during the S phase.

Results

ATM is required for proper degradation of Cdt1 during the unperturbed S phase

We established T98G cells stably expressing shRNA targeting ATM (referred to as T98G-ATMRi2) or luciferase as a control and investigated the effects of ATM inhibition on kinetics of various cell cycle- and DNA replication-related proteins during the cell cycle (**Fig. 1A**). In T98G–ATMRi2 cells, expression of ATM protein was reduced by ~90% (**Fig. 1A**), but cell cycle progression was delayed only slightly as compared with the

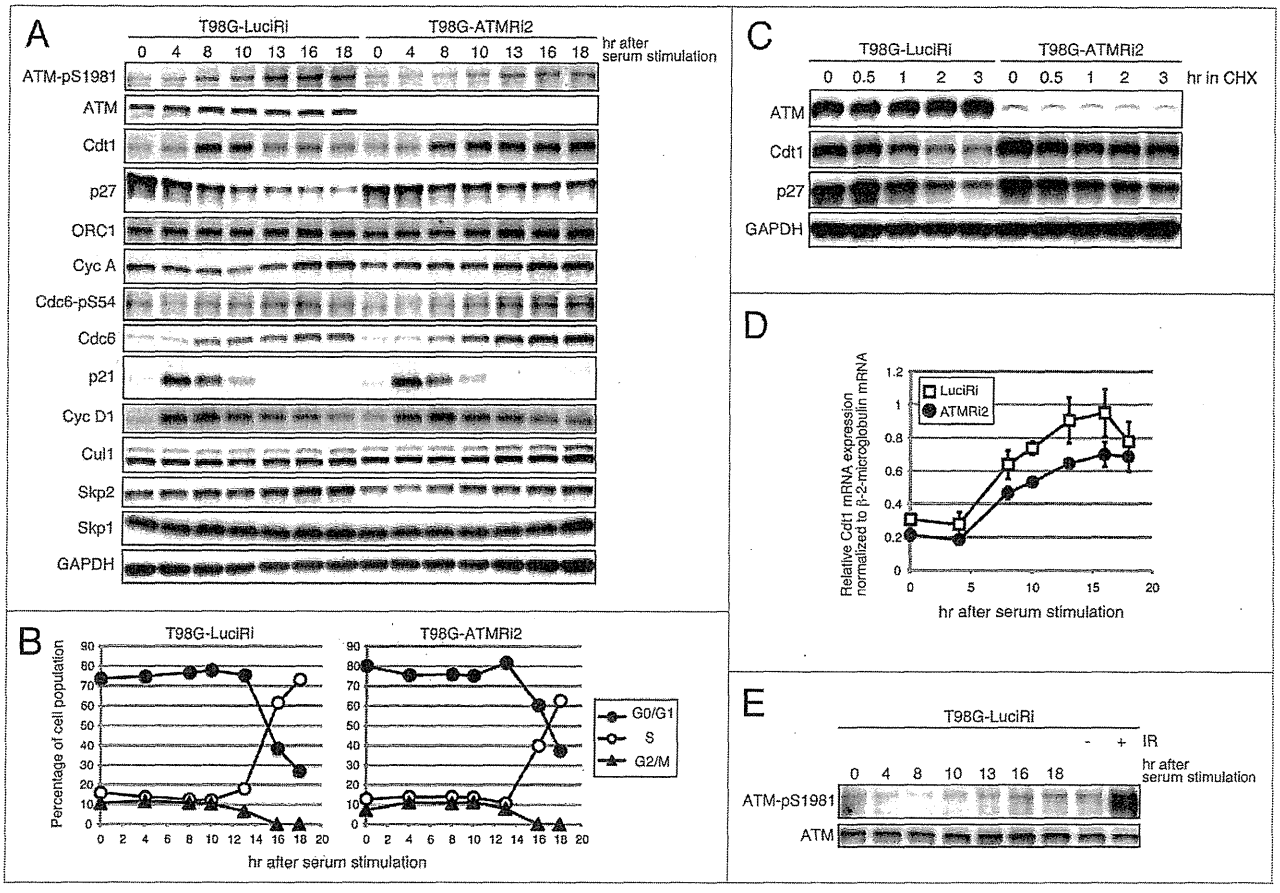

Figure 1. ATM is moderately auto-phosphorylated at Ser1981 in a cell cycle-dependent manner and required for appropriate degradation of Cdt1 and $p27^{Kip1}$ during the unperturbed S phase in T98G cells. (**A and B**) T98G cells expressing an shRNA targeting ATM (ATMRi2) or a control shRNA (LuciRi) were arrested in G_0 by serum starvation and then released into the cell cycle by serum addition. Cells were harvested at the indicated times and subjected to immunoblotting analysis (**A**) and flow cytometry (**B**). The percentage of cells in G_0/G_1, S, and G_2/M is shown by filled circle, open circle and filled triangle, respectively. (**C**) Cdt1 and $p27^{Kip1}$ is stabilized in ATM-silenced T98G cells. Cycloheximide (50 μg/ml) was added at 10 h after serum stimulation, and then the cells were harvested at the indicated times. (**D**) ATM silencing does not affect Cdt1 mRNA levels. Total RNAs were prepared from cells treated as in (**A**), and the levels of Cdt1 mRNA were determined by quantitative RT-PCR. (**E**) Phosphorylation of ATM at Ser1981 during the S phase is moderately induced compared with that induced in response to DNA damage. T98G-LuciRi cells were exposed to 5 Gy IR and harvested 30 min later (IR+) and subjected to immunoblotting analysis with protein lysates shown in (**A**). The data were obtained by short exposure compared with the data shown in (**A**).

control (Fig. 1B). We found cell cycle-dependent regulation of Cdt1 protein to be impaired by ATM inhibition. Thus, in control cells, Cdt1 protein levels were low in G_0, accumulated by 8 h after serum stimulation, and decreased remarkably after 13 h (Fig. 1A), coincident with the start of the S phase (Fig. 1B). This pattern of Cdt1 regulation is in agreement with previous findings.[14] In contrast, Cdt1 levels in ATM-silenced cells remained constant (Fig. 1A) in spite of the almost unimpeded S phase progression (Fig. 1B). Interestingly, downregulation of $p27^{Kip1}$ during the S phase was also impaired by ATM inhibition (Fig. 1A). The kinetics of cyclin A, Cdc6, ORC1, cyclin D1, and $p21^{WAF1}$ protein levels were unaffected (Fig. 1A). In addition, phosphorylation of Cdc6 at Ser54 by cyclin E/Cdk2 and cyclin A/Cdk2 occurred with similar kinetics (Fig. 1A), suggesting both kinases were properly activated in ATM-silenced cells. Essentially the same results were obtained with another shRNA targeting ATM (ATMRi4) (Fig. S1).

To determine whether ATM inhibition affect the stability of the Cdt1 and $p27^{Kip1}$ proteins, cycloheximide (CHX) was added to the ATMRi2 and control T98G cells at 10 h after serum stimulation and the protein levels were monitored (Fig. 1C). The data revealed that ATM inhibition stabilizes Cdt1 and $p27^{Kip1}$ proteins. We also found that ATM inhibition does not affect Cdt1 mRNA levels (Fig. 1D). Taken together, these results strongly indicate that ATM inhibition impedes the timely degradation of Cdt1 and $p27^{Kip1}$ proteins during the S phase in T98G cells.

ATM deficiency increases production of ROS (reactive oxygen species) in several cell types.[15,16] To ascertain whether Cdt1 deregulation by ATM inhibition is associated with aberrant ROS production, the levels were examined. In T98G cells, the ROS levels were not changed by ATM inhibition (Fig. S2A). In addition, treatment with antioxidant N-acetyl L-cysteine (NAC) did not prevent the inhibition of Cdt1 and $p27^{Kip1}$ degradation, in spite of efficient reduction of intracellular ROS (Fig. S2). Therefore, ROS is presumably not involved in the observed phenomena.

Using human foreskin fibroblasts immortalized with telomerase (HFF2/T), we further confirmed the novel function of ATM. Similar to T98G cells, whereas Cdt1 proteins were accumulated after serum stimulation and then decreased significantly upon entry into S phase in control cells, ATM silencing led to accumulation during S phase (Fig. 2A and B). On the other hand, the kinetics of $p27^{Kip1}$ protein levels were almost the same in control and ATM-silenced cells (Fig. 2A and B). In addition, we also found that Cdt1 and $p27^{Kip1}$ proteins remain abundant during the S phase in ATM-deficient

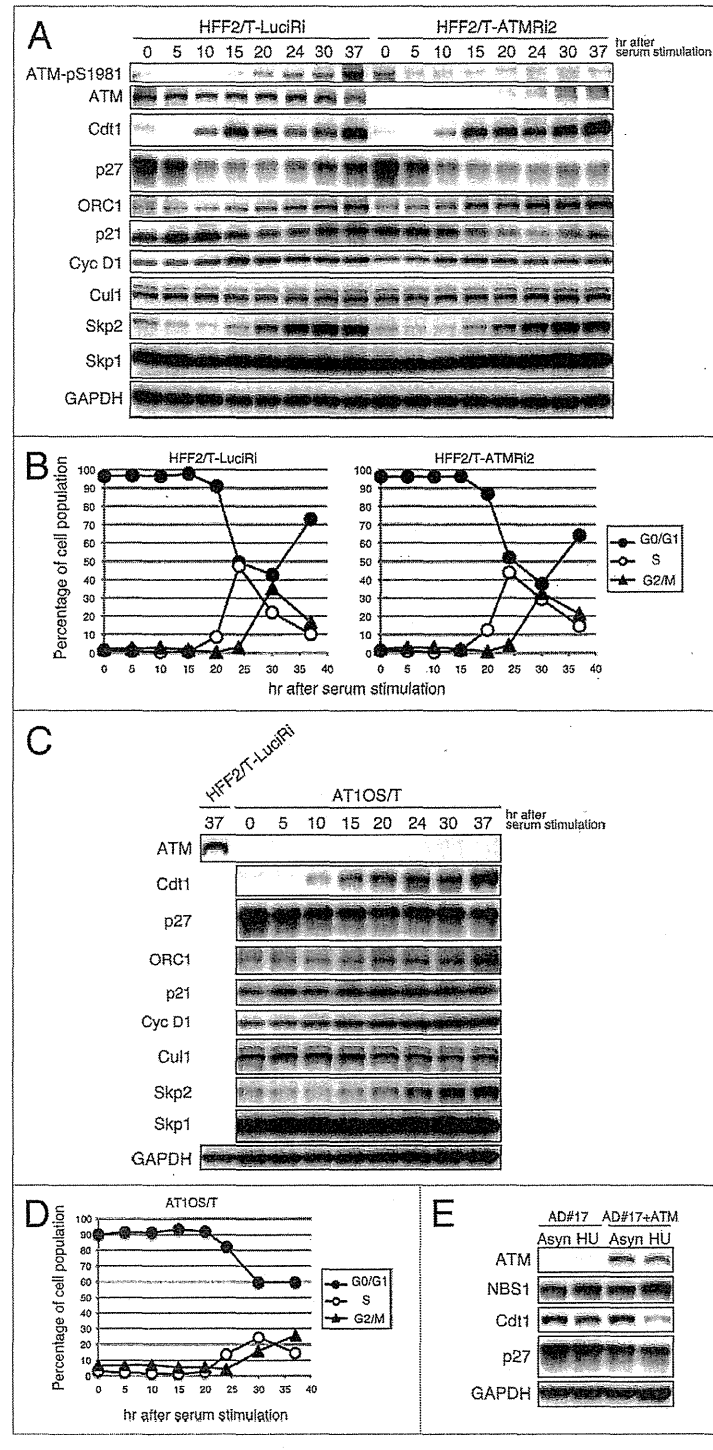

Figure 2. Involvement of ATM in Cdt1 regulation during the unperturbed S phase in human fibroblasts. (**A and B**) ATM is moderately auto-phosphorylated at Ser1981 in a cell cycle-dependent manner, and its silencing impairs Cdt1 downregulation during the S phase in HFF2/T cells. Cells expressing an ATMRi2 shRNA or a control shRNA (LuciRi) were synchronized and analyzed as in **Figure 1A and B.** (**C and D**) Cdt1 downregulation during the S phase is compromised in AT1OS/T, AT-derived fibroblasts. Cells were synchronized and analyzed as above. (**E**) Cdt1 deregulation during the S phase in AT-derived cells is alleviated by re-introduction of ATM. AD#17, another AT-derived fibroblast line, and its derivative reconstituted with ATM (AD#17+ATM), were treated with 2.5 mM hydroxyurea for synchronization in S phase (HU) or left untreated (Asyn) for 24 h and then analyzed by immunoblotting.

AT1OS/T cells (Fig. 2C and D). Furthermore, we examined a set of other AT-derived fibroblasts (AD#17), and their derivatives reconstituted with ATM (AD#17+ATM) for Cdt1 and $p27^{Kip1}$ protein levels upon synchronization in S phase by hydroxyurea (HU) treatment. In AD#17 cells, Cdt1 levels remained high upon HU treatment (Fig. 2E). The inappropriate accumulation of Cdt1 in S phase was abrogated by ATM add-back (Fig. 2E). HU treatment primarily blocks DNA replication fork progression and activates the ATR-Chk1 pathway. After the prolonged fork block, DSB is induced and the ATM-Chk2 pathway is activated. As mentioned below, Cdt1 is rapidly degraded upon DNA damage, which is mediated by PCNA-Cul4-$DDB1^{Cdt2}$ ubiquitin ligase but independent of ATM (ref. 17; Fig. S3). Because Cdt1 was not degraded in HU-treated AD#17 cells (Fig. 2E), abundant DSB may not be induced under the experimental conditions. Thus, the results of AD#17 and AD#17+ATM cells are consistent with the notion that degradation of Cdt1 during S phase is dependent on ATM. On the other hand, the protein levels of $p27^{Kip1}$ did not change on HU treatment in either AD#17 or AD#17+ATM cells.

Taken together, these data demonstrate that ATM protein is required for the proper degradation of Cdt1 during the S phase. At least in certain cell types, it may also be involved in degradation of $p27^{Kip1}$ during the S phase.

ATM kinase activity and NBS1 are required for the ATM-mediated Cdt1 regulation

We examined whether ATM could be activated during the S phase using ATM Ser1981 phosphorylation as an index,[7] and found that ATM Ser1981 is significantly phosphorylated during the S phase in T98G cells (Fig. 1A; Fig. S1), although the levels were low compared with those induced by 5 Gy IR (Fig. 1E). ATM phosphorylation at Ser1981 during the S phase was also observed in HFF2/T cells (Fig. 2A).

Given that ATM is activated during the S phase, we examined whether ATM kinase activity is involved in the Cdt1 regulation. To this end, quiescent T98G cells were released into the cell cycle by serum in the presence of an ATM-specific kinase inhibitor, KU-55933. KU-55933 treatment resulted in prevention of Cdt1 downregulation during the S phase, with inhibition of ATM Ser1981 phosphorylation (Fig. 3A and B). In contrast, $p27^{Kip1}$ protein was only slightly affected by the treatment. We also examined possible involvement of ATR in the Cdt1 regulation using an ATR specific kinase inhibitor, VE-821.[18] However, VE-821 did not affect Cdt1 downregulation (Fig. S4).

The MRN complex is required for ATM activation.[19] To investigate its requirement for ATM-dependent regulation of Cdt1, T98G cells were transfected with NBS1 siRNA and then synchronized. As shown in Figure 3C and D, decrease in Cdt1 protein levels during the S phase was significantly suppressed in NBS1-silenced cells. In contrast, the kinetics of $p27^{Kip1}$ were similar in both control and NBS1-silenced cells. We also examined Cdt1 and $p27^{Kip1}$ protein levels upon

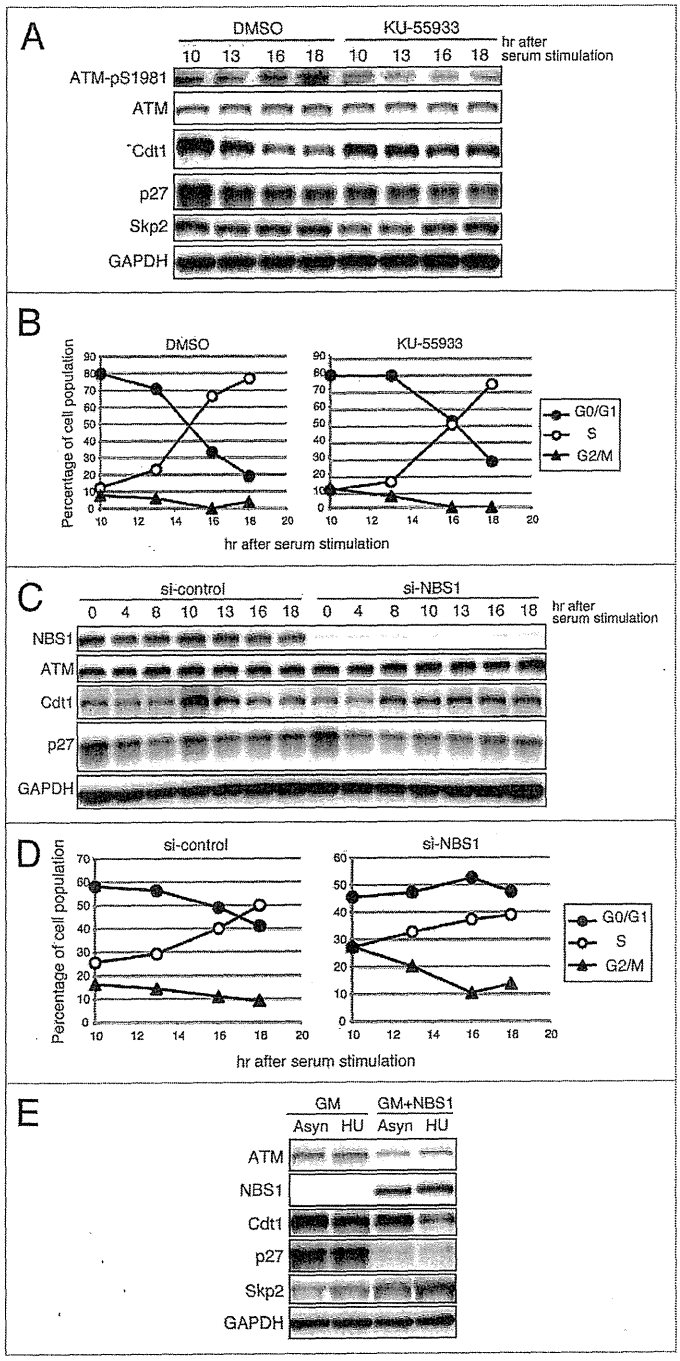

Figure 3. ATM kinase activity and NBS1 are required for Cdt1 regulation during the unperturbed S phase. (**A and B**) Inhibition of ATM kinase activity with KU-55933 impairs Cdt1 downregulation during the S phase in T98G cells. Cells were serum starved, pre-treated with 10 μM KU-55933, and then reentered into the cell cycle. Cells were harvested at the indicated times and subjected to immunoblotting (**A**) and flow cytometry (**B**). (**C and D**) NBS1 silencing impairs Cdt1 downregulation during the S phase in T98G cells. Cells were transfected with NBS1 or control siRNAs, synchronized, and harvested at the indicated times after reentry into the cell cycle for immunoblotting (**C**) and flow cytometry (**D**). (**E**) Cdt1 deregulation during the S phase in NBS-derived cells is alleviated by re-introduction of NBS1. NBS1-deficient cells (GM) and the reconstituted cells with NBS1 (GM+NBS1) were treated with 2.5 mM HU for synchronization in S phase (HU) or left untreated (Asyn) for 11 h and then analyzed by immunoblotting.

S-phase synchronization by HU treatment in NBS1-deficient cells (GM7166) and their derivatives reconstituted with NBS1 (GM7166+NBS1). Cdt1 protein levels decreased significantly with HU treatment in GM7166+NBS1 cells, whereas they were unchanged in GM7166 (**Fig. 3E**). In contrast, the protein levels of $p27^{Kip1}$ in GM7166+NBS1 cells were very low as compared with parental GM7166 cells, irrespective of HU treatment. The reason for the unexpected response of $p27^{Kip1}$ to NBS1 is not clear at present.

Taken together, these observations demonstrate that kinase activity of ATM and NBS1 are required for proper Cdt1 degradation during the S phase. On the other hand, it seems likely that the effects of ATM pathways on the regulation of $p27^{Kip1}$ during the S phase are more complex and diverse, depending on the cell types.

ATM is involved in the regulation of Skp2 as a critical mediator of Cdt1 degradation in T98G cells

As mentioned above, degradation of Cdt1 during the S phase is mediated by Cdk-SCF^{Skp2} and PCNA-Cul4-$DDB1^{Cdt2}$ ubiquitin ligases, whereas degradation of Cdt1 after DNA damage is mediated by PCNA-Cul4-$DDB1^{Cdt2}$.[8,17,20,21] The extent of dependence on the either degradation machinery during the S phase appears different among cell types.[11,21,22]

Consistent with a previous report,[17] IR- and UV-mediated Cdt1 proteolysis proved independent of ATM (**Fig. S3**). In addition, cell cycle regulation of $p21^{WAF1}$, another target of Cul4-$DDB1^{Cdt2}$ ubiquitin ligase, appeared unaffected by ATM inhibition (**Figs. 1A and 2A**; **Fig. S1**). Furthermore, $p27^{Kip1}$ is also regulated by SCF^{Skp2}.[23] Therefore, ATM might affect the SCF^{Skp2}-mediated pathway. It was reported that ATM mediates full activation of Akt in response to insulin or DNA damage,[24-27] and several reports have demonstrated that Akt may regulate Skp2 function at both transcriptional and posttranscriptional levels.[28-31] Therefore, we investigated whether ATM inhibition might affect SCF^{Skp2} functions.

Levels of Cul1 and Skp1, 2 components of SCF^{Skp2}, remained constant throughout the cell cycle in T98G cells, which were not affected by ATM inhibition (**Fig. 1A**; **Fig. S1**). The Skp2

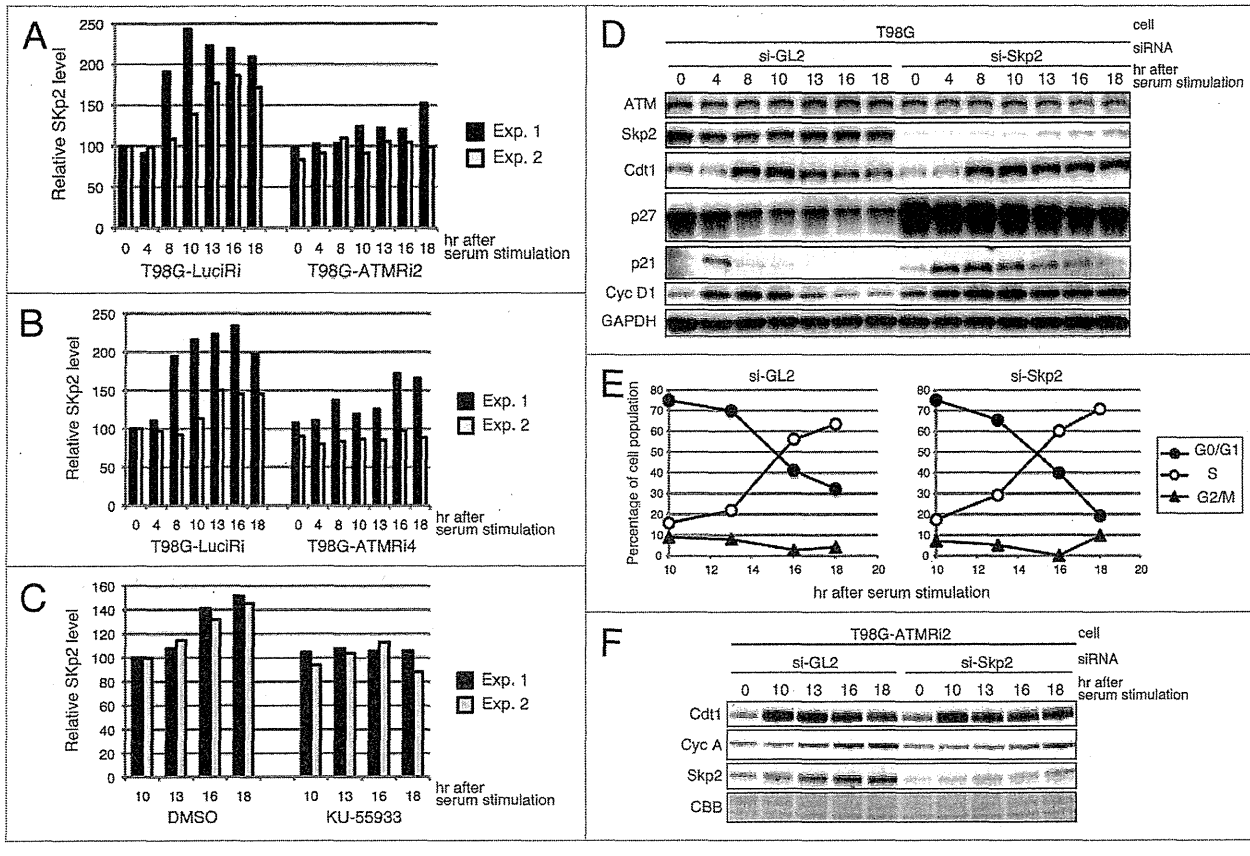

Figure 4. ATM is involved in the regulation of Skp2 levels during the unperturbed S phase in T98G cells. (**A–C**) Either ATM depletion or inhibition of its kinase activity leads to decrease in Skp2. The signal intensities of the Skp2 proteins in cells treated as in **Figure 1A**, **Figure S1A**, or **Figure 3A** were quantified and normalized to the signals for GAPDH. (**A**) Data for T98G-ATMRi2 cells. (**B**) Data for T98G-ATMRi4 cells. For (**A and B**), the graphs show values for Skp2 relative to the level in T98G-LuciRi cells at 0 h. (**C**) Data for KU-55933-treated cells. The graph shows values for Skp2 relative to the level in DMSO-treated cells at 10 h after serum stimulation. The black and gray bars indicate independent experiments No. 1 and No. 2, respectively. (**D and E**) Skp2 depletion upregulates Cdt1 and $p27^{Kip1}$ during the S phase in T98G cells. Cells were transfected with Skp2 or control siRNAs, synchronized, released into the cell cycle and analyzed as in **Figure 1A and B**. (**F**) Co-depletion of Skp2 does not further stabilize Cdt1 during the S phase in ATM-silenced T98G cells. T98G-ATMRi2 cells were transfected with Skp2 or control siRNAs, synchronized, released into the cell cycle, and analyzed as in (**D**). In these experiments, S-phase progression was monitored by accumulation of cyclin A.

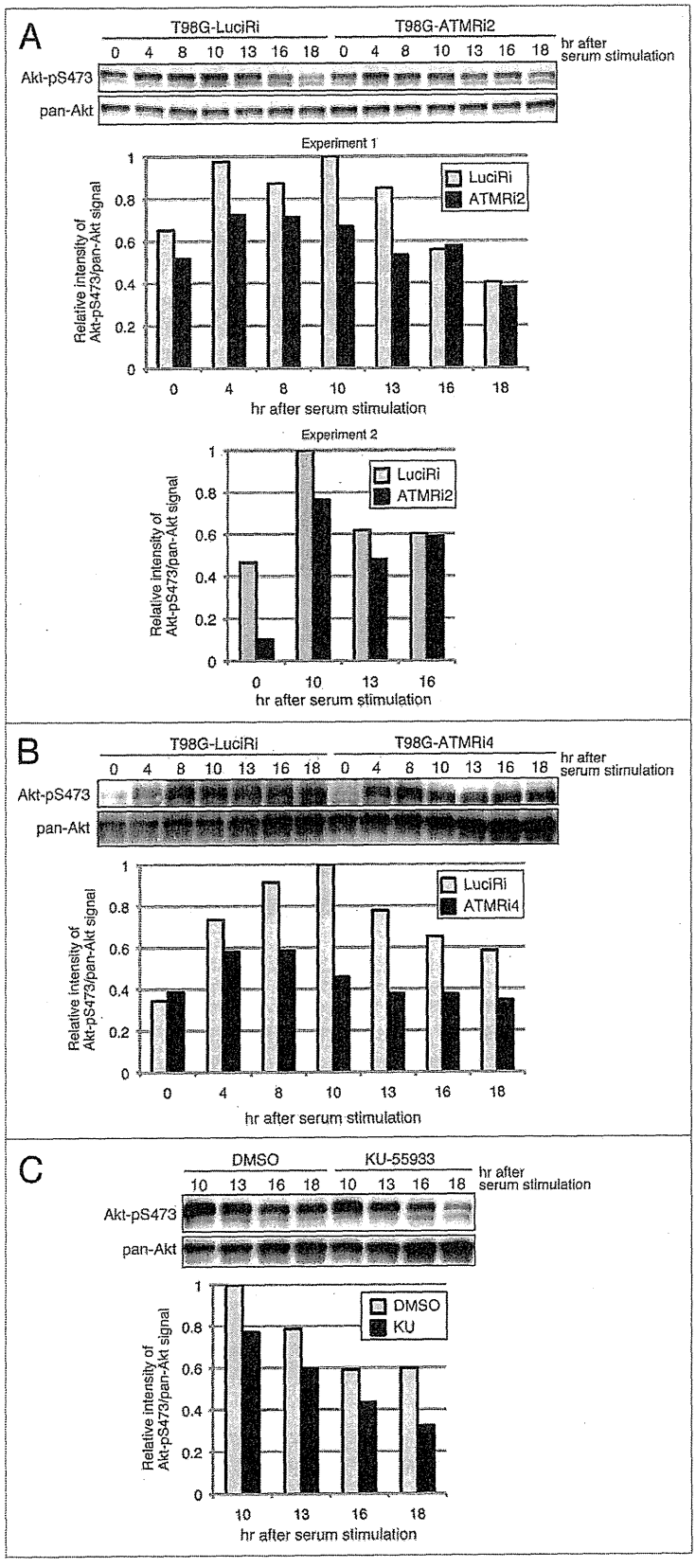

Figure 5A–C. ATM inhibition partially affects the Akt-SCF^{Skp2} pathway in T98G cells. (**A–C**) ATM silencing and inhibition of its kinase activity reduce Akt phosphorylation at Ser473. The cell lysates prepared as in **Figure 1A**, **Figure S1A**, and **Figure 3A**, respectively, were subjected to immunoblotting with pan-Akt and Ser473-phosphorylated Akt antibodies. The signal intensities of total Akt and the phosphorylated Akt were quantified, and the ratio of the phosphorylated Akt to total Akt was calculated. The graphs in (**A and B**) show values relative to that for T98G-LuciRi cells at 10 h after serum stimulation set at 1. The graph in (**C**) shows values relative to that of DMSO-treated cells at 10 h after serum stimulation set at 1.

protein level is controlled by APC/C^{Cdh1}-mediated proteolysis during the G_1 phase.[32,33] Consistent with this, Skp2 levels were cell cycle-regulated in T98G cells, with increase in S phase (**Figs. 1A and 3A**; **Fig. S1**). Interestingly, accumulation of Skp2 during the S phase was partially delayed and inhibited by ATM silencing in T98G cells (**Fig. 4A and B**, see also **Fig. 1A**; **Fig. S1** for some of the original data used for quantification). Similar findings were also obtained with KU-55933 (**Fig. 4C**, see also **Fig. 3A** as one of the original data used for quantification). Moreover, Skp2 level during the S phase in NBS1-deficient cells was lower than that in NBS1-reconstituted cells (**Fig. 3E**).

Given that Cdt1 deregulation by ATM suppression may be attributable to, at least partly, decrease in Skp2 levels, we examined whether Skp2 silencing affects Cdt1 degradation during the S phase in T98G cells (**Fig. 4D**). As expected, Cdt1 protein levels remained constant during the S phase in Skp2-silenced T98G cells (**Fig. 4D**). Thus, although Cdt1 degradation is controlled by 2 ubiquitin ligases, SCF^{Skp2} and $Cul4\text{-}DDB1^{Cdt2}$, the former may be predominant in T98G cells. In Skp2-silenced cells, $p27^{Kip1}$ increased quite remarkably throughout the cell cycle (**Fig. 4D**), suggesting its strong dependence on the Skp2 protein. Therefore, in certain cell types, such as T98G, partial decrease in Skp2 levels by ATM silencing may lead to $p27^{Kip1}$ accumulation during S phase. Cyclin D1 and $p21^{WAF1}$ are also substrates of SCF^{Skp2},[23] although also regulated by other ubiquitin ligases, and actually their degradation was prevented by Skp2 silencing (**Fig. 4D**). However, neither cyclin D1 nor $p21^{WAF1}$ protein levels were changed by ATM silencing (**Fig. 1A**; **Fig. S1**). It is possible that partial decrease in Skp2 by ATM silencing may be insufficient for significant stabilization of these proteins. We also examined whether co-silencing of Skp2 further stabilizes Cdt1 during the S phase in ATM-silenced cells. Simultaneous depletion of Skp2 did not further stabilize Cdt1 in T98G-ATMRi2 cells (**Fig. 4F**), in line with the notion that Cdt1 stabilization by ATM inhibition is attributed to Skp2 inhibition. Finally, we investigated whether ATM silencing affects the binding of Skp2 to Skp1 and Cul1 or the intracellular localization of Skp2. However, no significant

findings were obtained (Fig. S5). Taken together, these results suggest that ATM affects Cdt1 degradation through, at least partly, maintaining Skp2 levels during the S phase in T98G cells.

ATM inhibition partially affects the Akt-SCF^{Skp2} pathway in T98G cells

Since previous reports indicated possible interplay between ATM and Akt,[24-27] we next examined whether ATM function is associated with Akt activation during the cell cycle. When quiescent T98G-LuciRi cells were stimulated with serum, phosphorylation of Akt at Ser473, indicative of Akt activation,[34] was increased and then decreased gradually at 13 h after serum addition (Fig. 5A and B). When ATM was silenced with ATMRi2 or ATMRi4, such Akt phosphorylation was partially suppressed (Fig. 5A and B). Similar phenomena were also observed in KU-55933-treated cells (Fig. 5C). A previous report showed physical interaction between ATM and Akt.[24] We also found that Akt can bind to ATM fragments fused to GST (data not shown).

We then investigated whether Akt silencing indeed affects Cdt1 degradation during S phase. Consistent with previous findings,[28-30,35] silencing of either Akt1, Akt2, or both, strongly decreased the protein level of Skp2 (Fig. 5D). In further agreement with previous reports,[28,31] we also observed physical interaction between Akt and Skp2 in co-immunoprecipitation assays and Skp2 upregulation in Akt-overexpressed cells (data not shown). As expected from the Skp2 reduction, p27^{Kip1} levels were remarkably increased in Akt-silenced cells (Fig. 5D). Unexpectedly, however, Akt silencing only modestly stabilized Cdt1 (Fig. 5D). The reason is not clear at present but some compensatory pathway(s) might be activated upon Akt depletion. In the study using siRNA-mediated Akt silencing and subsequent cell cycle

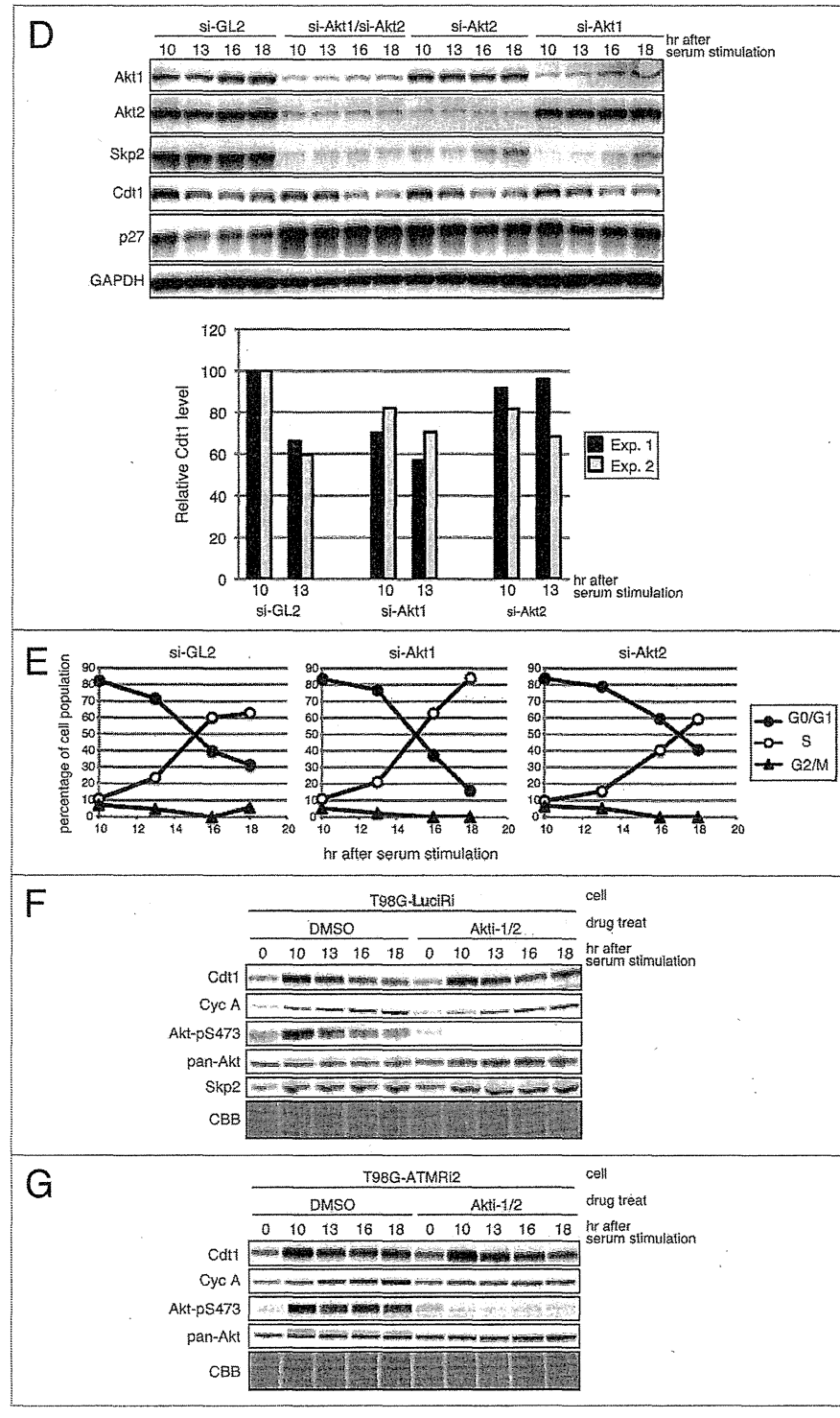

Figure 5D–G. ATM inhibition partially affects the Akt-SCF^{Skp2} pathway in T98G cells. (**D and E**) Akt1 or Akt2 depletion affects Skp2-mediated Cdt1 and p27^{Kip1} degradation in T98G cells. Cells were transfected with siRNAs targeting Akt1, Akt2, or both, or control siRNA (si-GL2), serum starved, and then stimulated by serum. Cells were harvested at the indicated times for immunoblotting (**D**) and flow cytometry (**E**). (**D**) The signal intensities of the Cdt1 proteins were quantified and normalized to the signals for GAPDH. The graph shows the values relative to Cdt1 levels in control siRNA-treated cells at 10 h after serum stimulation. (**F**) Inhibition of Akt kinase activity with Akti-1/2 impairs Cdt1 downregulation during the S phase in T98G cells. Cells were treated with 10 μM Akti-1/2 at 9 h after cell cycle entry from G_0, and then harvested at the indicated times. In these experiments, S-phase progression was monitored by accumulation of cyclin A. (**G**) Co-inhibition of Akt with Akti-1/2 does not further stabilize Cdt1 during the S phase in ATM-silenced T98G cells. T98G-ATMRi2 cells were treated and analyzed as above.

synchronization, Akt function during G_1 progression is inevitably affected. To investigate the effect of Akt inhibition on Cdt1 regulation specifically in S phase, we utilized an Akt1/2 specific inhibitor, Akti-1/2.[36] Treatment of Akti-1/2 resulted in prevention of Cdt1 downregulation during the S phase, with inhibition of Akt Ser473 phosphorylation (Fig. 5F). Unexpectedly, however, the protein level of Skp2 was not changed. It is possible that the function of Skp2 rather than the protein level is impaired under these experimental conditions. Moreover, we examined the effect of Akt co-inhibition on Cdt1 stabilization during the S phase in ATM-silenced T98G cells. Inhibition of Akt with Akti-1/2 did not further stabilize Cdt1 in T98G-ATMRi2 cells (Fig. 5G). Together, these observations suggest that ATM inhibition may at least partially affect the Akt-SCF^{Skp2}-Cdt1 pathway.

ATM inhibition renders cells hypersensitive to induction of re-replication

Cdt1 deregulation leads to chromosomal damage, including re-replication.[9-13,37] We therefore examined whether the stabilization of Cdt1 by ATM silencing leads to re-replication. Flow cytometry analyses revealed that re-replicated population (defined by a DNA content higher than 4N) in AT cells is 1.5-fold that in ATM-complemented cells (Fig. 6A and B). If increase in re-replication in ATM-deficient cells is attributable to Cdt1 upregulation during the S phase, then it would be enhanced by co-overexpression of Cdc6.[9,11] Therefore, we overexpressed Cdc6 in T98G-ATMRi2 and control T98G-LuciRi cells. Even in an asynchronous population, increase in Cdt1 levels was detectable in ATMRi2 cells, and Cdc6 overexpression was confirmed in both cells (Fig. 6C). The induction of re-replication in ATMRi2 cells was similar to that in control cells. However, Cdc6 overexpression enhanced re-replication induction only in T98G-ATMRi2 cells (Fig. 6D). Thus, ATM deficiency rendered cells hypersensitive to induction of re-replication, indicating the importance of the novel ATM function in maintenance of genome stability.

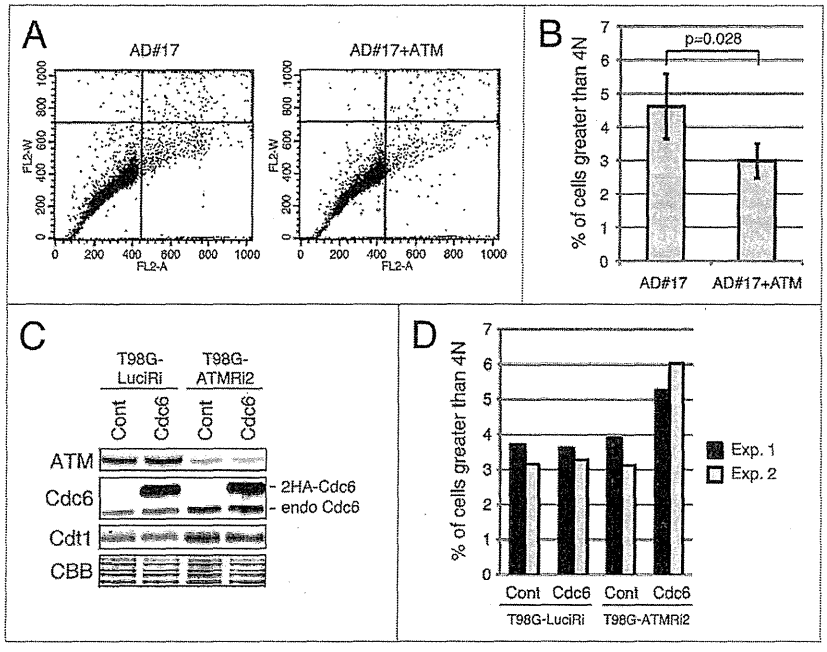

Figure 6. ATM inhibition renders cells hypersensitive to induction of re-replication. (**A and B**) The AT-derived AD#17, and its derivative reconstituted with ATM (AD#17+ATM), were subjected to flow cytometry. (**A**) In these diagrams, the *x*-axis is FL2-A representing whole PI signals and thus DNA content, and the *y*-axis is FL2-W representing duration of PI signals. Dots with higher FL2-W signals that result from aggregated cells or cell debris were excluded from measurement of re-replicated cells. (**B**) The means and SDs of the percentages of re-replicated cells (DNA content higher than 4N) from 3 independent experiments are shown. (**C and D**) T98G-LuciRi and ATM-silenced T98G-ATMRi2 cells were infected with retroviruses expressing 2HA-Cdc6 or with control retroviruses, and selected with puromycin (1 μg/ml). At 4 d after infection, cells were subjected to immunoblotting (**C**) and flow cytometry (**D**). In (**D**), percentages of re-replicated cells are shown.

Discussion

ATM is involved in appropriate degradation of Cdt1 during the unperturbed S phase

An ATM requirement for timely degradation of Cdt1 during the S phase was observed in several different systems, i.e., T98G, HFF2/T, and 2 different AT patient-derived cells (Figs. 1 and 2; Fig. S1). This ATM function requires its kinase activity and NBS1 (Fig. 3). Indeed, ATM activation indicated by Ser1981 phosphorylation is detected during the S phase both in T98G and HFF2/T cells (Figs. 1A and 2A; Fig. S1A). However, the mechanisms by which ATM is moderately activated during the S phase remain to be clarified. There are several non-exclusive possibilities. One is that the replication process affects the chromatin architecture, triggering ATM activation. Alternatively, replication forks accidentally encounter endogenously generated chromatin stresses, leading to transient DSB induction. At telomeres, ATM activation is generally suppressed. However, ATM may be appropriately activated during the S phase to maintain telomere structure.[38-40] It was previously reported that MRN is required for suppression of re-replication induced by overexpression of Cdt1, and this mechanism is mediated by ATR.[12] However, ATR is not required for Cdt1 regulation during the S phase (Fig. S4).

ATM functions to prohibit re-replication

Cdt1 deregulation induces re-replication and/or chromosomal damage, leading to chromosomal instability.[9-11,13,37] In non-transformed cells, although Cdt1 overexpression induces only small amounts of re-replication, co-expression of ORC1 or Cdc6 robustly enhances re-replication.[11] Therefore, it is conceivable that undesired Cdt1 upregulation in ATM-inhibited cells may cause deleterious insult. Actually, the re-replicated cell population is significantly increased in an AT-derived cell line, which could be corrected by ATM reintroduction (Fig. 6A and B). More importantly, Cdc6 overexpression enhanced re-replication in ATM-silenced T98G cells (Fig. 6C

and D), indicating that Cdt1 upregulation by ATM inhibition in fact predisposes cells to re-replication. Thus, the novel function of ATM described here may have a critical role in genome maintenance.

Signaling pathways from ATM to Cdt1

Whereas it seems clear that ATM participates in Cdt1 regulation, the involved signaling pathways appear complicated and are not fully understood. It seems likely that multiple parallel pathways contribute to the novel ATM function.

At least in T98G cells, the ATM-Akt-SCF^{Skp2} axis may be one pathway. The evidence includes: (1) ATM inhibition, at least partially, downregulates Skp2 protein levels (**Fig. 4A–C**); (2) Skp2 silencing stabilizes Cdt1 during the S phase (**Fig. 4D**); (3) ATM inhibition moderately inhibits Akt phosphorylation (**Fig. 5A–C**); (4) Akt silencing decreases the Skp2 protein levels (**Fig. 5D**), and, conversely, Akt overexpression increases (data not shown; refs. 28–30, and 35); and (5) Akt inhibition stabilizes Cdt1 during the S phase (**Fig. 5F**). In addition, in agreement with previous data,[24,28,31] (6) we also found ATM–Akt and Akt–Skp2 physical interactions (data not shown). This notion is also supported by the fact that co-silencing of Skp2 or co-inhibition of Akt in ATM-silenced T98G cells does not induce further stabilization of Cdt1 (**Figs. 4F and 5G**). However, even in T98G cells, there are some apparently contradictory findings; e.g., in spite of significant suppression of Skp2 protein levels in Akt-silenced cells, Cdt1 is only partially stabilized during the S phase (**Fig. 5D**), and neither cyclin D1 nor p21^{WAF1} protein levels, regulated by SCF^{Skp2},[23] are changed by ATM silencing (**Fig. 1A; Fig. S1**). Manipulation of one pathway could activate compensatory parallel pathways in some cases. Nevertheless, these findings appears in line with previous reports showing that ATM mediates full activation of Akt in response to insulin or DNA damage,[24-27] and that Akt may regulate Skp2 at both transcriptional and posttranscriptional levels.[28-31] It is also reported that Mre11 promotes Akt phosphorylation in response to DNA DSBs.[41] Unfortunately, to date, it remains completely unclear how ATM regulates Akt. A biological relevance of Akt-mediated Skp2 regulation has been proposed, but discussion continues.[28-31,42-44] It is possible that Akt regulation of Skp2 is cell type- and/or context-dependent.

In other cell systems, the pathway by which ATM regulates Cdt1 is more obscure and remains to be determined. For instance, in HFF2/T cells, ATM silencing upregulates the Cdt1 levels during the S phase without reducing the Skp2 protein levels (**Fig. 2A**). In this case, ATM might affect Skp2 protein function(s) rather than the levels.

ATM involvement in p27^{Kip1} regulation during the unperturbed S phase

p27^{Kip1} is an important Cdk inhibitor that is elaborately regulated during the cell cycle and cell differentiation. This is executed at multiple levels and in a cell type- and/or context-dependent manner.[45,46] For example, at least 4 ubiquitin ligases control the stability. SCF^{Skp2} is one representative ubiquitin ligase that controls p27^{Kip1} dependent on Cdk phosphorylation. We found here that, at least in T98G cells, ATM participates in regulation of p27^{Kip1} stability during the S phase (**Fig. 1**). In this context, the ATM-Akt-SCF^{Skp2} axis may play a role (**Figs. 4, 5A–C, and 5D–G**), as well as in the regulation of Cdt1, with difference of a low requirement of ATM kinase activity and NBS1. However, in other cell types, ATM does not appear to affect p27^{Kip1} protein levels (**Fig. 2**). This may be due to complexities in p27^{Kip1} regulations. In addition, the pathophysiological relevance of inappropriate p27^{Kip1} upregulation in some ATM-deficient cells remains to be elucidated in the future.

Materials and Methods

Cells

Cells used are described in **Supplementary Materials and Methods**. Cells were grown in Dulbecco modified Eagle medium (DMEM) with 8% fetal calf serum. T98G cells were synchronized in quiescence by serum starvation for 48 h, followed by reentry into the cell cycle by incubation in DMEM with 15% serum. Synchronization of HFF2/T and AT1OS/T cells into quiescence was achieved by contact inhibition and sequential serum starvation. The inhibitors used are detailed in **Supplementary Materials and Methods**.

Transfection

T98G cells (9×10^4 /well in 6-well plates) were transfected with 40 pmol of siRNA using Lipofectamine RNAiMAX (Invitrogen) according to the manufacturer's protocol. The sequences of siRNAs are described in **Supplementary Materials and Methods**.

FACS

Cells were stained with propidium iodide (PI), and analyzed with a Becton Dickinson FACS Calibur.

Details of other materials and methods are described in **Supplementary Materials and Methods**.

Disclosure of Potential Conflicts of Interest

No potential conflicts of interest were disclosed.

Acknowledgments

We thank Kum Kum Khanna (Queensland Institute of Medical Research, Australia) for plasmids of GST-truncated ATM. We appreciate for the technical supports from the Research Support Center, Graduate School of Medical Sciences, Kyushu University.

Financial support

Ministry of Education, Culture, Sports, Science and Technology of Japan (17080013 and 24650622) for M Fujita.

Supplemental Materials

Supplemental materials may be found here:
www.landesbioscience.com/journals/cc/article/27274

References

1. Bartek J, Lukas J. Chk1 and Chk2 kinases in checkpoint control and cancer. Cancer Cell 2003; 3:421-9; PMID:12781359; http://dx.doi.org/10.1016/S1535-6108(03)00110-7
2. Kastan MB, Bartek J. Cell-cycle checkpoints and cancer. Nature 2004; 432:316-23; PMID:15549093; http://dx.doi.org/10.1038/nature03097
3. Nyberg KA, Michelson RJ, Putnam CW, Weinert TA. Toward maintaining the genome: DNA damage and replication checkpoints. Annu Rev Genet 2002; 36:617-56; PMID:12429704; http://dx.doi.org/10.1146/annurev.genet.36.060402.113540
4. Cam H, Easton JB, High A, Houghton PJ. mTORC1 signaling under hypoxic conditions is controlled by ATM-dependent phosphorylation of HIF-1α. Mol Cell 2010; 40:509-20; PMID:21095582; http://dx.doi.org/10.1016/j.molcel.2010.10.030
5. Guo Z, Kozlov S, Lavin MF, Person MD, Paull TT. ATM activation by oxidative stress. Science 2010; 330:517-21; PMID:20966255; http://dx.doi.org/10.1126/science.1192912
6. Hinz M, Stilmann M, Arslan SC, Khanna KK, Dittmar G, Scheidereit C. A cytoplasmic ATM-TRAF6-cIAP1 module links nuclear DNA damage signaling to ubiquitin-mediated NFκB activation. Mol Cell 2010; 40:63-74; PMID:20932475; http://dx.doi.org/10.1016/j.molcel.2010.09.008
7. Bakkenist CJ, Kastan MB. DNA damage activates ATM through intermolecular autophosphorylation and dimer dissociation. Nature 2003; 421:499-506; PMID:12556884; http://dx.doi.org/10.1038/nature01368
8. Fujita M. Cdt1 revisited: complex and tight regulation during the cell cycle and consequences of deregulation in mammalian cells. Cell Div 2006; 1:22; PMID:17042960; http://dx.doi.org/10.1186/1747-1028-1-22
9. Vaziri C, Saxena S, Jeon Y, Lee C, Murata K, Machida Y, Wagle N, Hwang DS, Dutta A. A p53-dependent checkpoint pathway prevents rereplication. Mol Cell 2003; 11:997-1008; PMID:12718885; http://dx.doi.org/10.1016/S1097-2765(03)00099-6
10. Sugimoto N, Kitabayashi I, Osano S, Tatsumi Y, Yugawa T, Narisawa-Saito M, Matsukage A, Kiyono T, Fujita M. Identification of novel human Cdt1-binding proteins by a proteomics approach: proteolytic regulation by APC/CCdh1. Mol Biol Cell 2008; 19:1007-21; PMID:18162579; http://dx.doi.org/10.1091/mbc.E07-09-0859
11. Sugimoto N, Yoshida K, Tatsumi Y, Yugawa T, Narisawa-Saito M, Waga S, Kiyono T, Fujita M. Redundant and differential regulation of multiple licensing factors ensures prevention of re-replication in normal human cells. J Cell Sci 2009; 122:1184-91; PMID:19339550; http://dx.doi.org/10.1242/jcs.041889
12. Lee AY, Liu E, Wu X. The Mre11/Rad50/Nbs1 complex plays an important role in the prevention of DNA rereplication in mammalian cells. J Biol Chem 2007; 282:32243-55; PMID:17715134; http://dx.doi.org/10.1074/jbc.M705486200
13. Tatsumi Y, Sugimoto N, Yugawa T, Narisawa-Saito M, Kiyono T, Fujita M. Deregulation of Cdt1 induces chromosomal damage without rereplication and leads to chromosomal instability. J Cell Sci 2006; 119:3128-40; PMID:16835273; http://dx.doi.org/10.1242/jcs.03031
14. Nishitani H, Taraviras S, Lygerou Z, Nishimoto T. The human licensing factor for DNA replication Cdt1 accumulates in G1 and is destabilized after initiation of S-phase. J Biol Chem 2001; 276:44905-11; PMID:11555648; http://dx.doi.org/10.1074/jbc.M105406200
15. Kim J, Wong PK. Oxidative stress is linked to ERK1/2-p16 signaling-mediated growth defect in ATM-deficient astrocytes. J Biol Chem 2009; 284:14396-404; PMID:19321450; http://dx.doi.org/10.1074/jbc.M808116200
16. Ito K, Takubo K, Arai F, Satoh H, Matsuoka S, Ohmura M, Naka K, Azuma M, Miyamoto K, Hosokawa K, et al. Regulation of reactive oxygen species by Atm is essential for proper response to DNA double-strand breaks in lymphocytes. J Immunol 2007; 178:103-10; PMID:17182545
17. Higa LA, Mihaylov IS, Banks DP, Zheng J, Zhang H. Radiation-mediated proteolysis of CDT1 by CUL4-ROC1 and CSN complexes constitutes a new checkpoint. Nat Cell Biol 2003; 5:1008-15; PMID:14578910; http://dx.doi.org/10.1038/ncb1061
18. Reaper PM, Griffiths MR, Long JM, Charrier JD, Maccormick S, Charlton PA, Golec JM, Pollard JR. Selective killing of ATM- or p53-deficient cancer cells through inhibition of ATR. Nat Chem Biol 2011; 7:428-30; PMID:21490603; http://dx.doi.org/10.1038/nchembio.573
19. Uziel T, Lerenthal Y, Moyal L, Andegeko Y, Mittelman L, Shiloh Y. Requirement of the MRN complex for ATM activation by DNA damage. EMBO J 2003; 22:5612-21; PMID:14532133; http://dx.doi.org/10.1093/emboj/cdg541
20. Hu J, McCall CM, Ohta T, Xiong Y. Targeted ubiquitination of CDT1 by the DDB1-CUL4A-ROC1 ligase in response to DNA damage. Nat Cell Biol 2004; 6:1003-9; PMID:15448697; http://dx.doi.org/10.1038/ncb1172
21. Nishitani H, Sugimoto N, Roukos V, Nakanishi Y, Saijo M, Obuse C, Tsurimoto T, Nakayama KI, Nakayama K, Fujita M, et al. Two E3 ubiquitin ligases, SCF-Skp2 and DDB1-Cul4, target human Cdt1 for proteolysis. EMBO J 2006; 25:1126-36; PMID:16482215; http://dx.doi.org/10.1038/sj.emboj.7601002
22. Arias EE, Walter JC. PCNA functions as a molecular platform to trigger Cdt1 destruction and prevent re-replication. Nat Cell Biol 2006; 8:84-90; PMID:16362051; http://dx.doi.org/10.1038/ncb1346
23. Frescas D, Pagano M. Deregulated proteolysis by the F-box proteins SKP2 and beta-TrCP: tipping the scales of cancer. Nat Rev Cancer 2008; 8:438-49; PMID:18500245; http://dx.doi.org/10.1038/nrc2396
24. Viniegra JG, Martínez N, Modirassari P, Hernández Losa J, Parada Cobo C, Sánchez-Arévalo Lobo VJ, Aceves Luquero CI, Alvarez-Vallina L, Ramón y Cajal S, Rojas JM, et al. Full activation of PKB/Akt in response to insulin or ionizing radiation is mediated through ATM. J Biol Chem 2005; 280:4029-36; PMID:15546863; http://dx.doi.org/10.1074/jbc.M410344200
25. Khalil A, Morgan RN, Adams BR, Golding SE, Dever SM, Rosenberg E, Povirk LF, Valerie K. ATM-dependent ERK signaling via AKT in response to DNA double-strand breaks. Cell Cycle 2011; 10:481-91; PMID:21263216; http://dx.doi.org/10.4161/cc.10.3.14713
26. Golding SE, Rosenberg E, Valerie N, Hussaini I, Frigerio M, Cockcroft XF, Chong WY, Hummersone M, Rigoreau L, Menear KA, et al. Improved ATM kinase inhibitor KU-60019 radiosensitizes glioma cells, compromises insulin, AKT and ERK prosurvival signaling, and inhibits migration and invasion. Mol Cancer Ther 2009; 8:2894-902; PMID:19808981; http://dx.doi.org/10.1158/1535-7163.MCT-09-0519
27. Li Y, Yang DQ. The ATM inhibitor KU-55933 suppresses cell proliferation and induces apoptosis by blocking Akt in cancer cells with overactivated Akt. Mol Cancer Ther 2010; 9:113-25; PMID:20053781; http://dx.doi.org/10.1158/1535-7163.MCT-08-1189
28. Gao D, Inuzuka H, Tseng A, Chin RY, Toker A, Wei W. Phosphorylation by Akt1 promotes cytoplasmic localization of Skp2 and impairs APCCdh1-mediated Skp2 destruction. Nat Cell Biol 2009; 11:397-408; PMID:19270695; http://dx.doi.org/10.1038/ncb1847
29. Reichert M, Saur D, Hamacher R, Schmid RM, Schneider G. Phosphoinositide-3-kinase signaling controls S-phase kinase-associated protein 2 transcription via E2F1 in pancreatic ductal adenocarcinoma cells. Cancer Res 2007; 67:4149-56; PMID:17483325; http://dx.doi.org/10.1158/0008-5472.CAN-06-4484
30. Barré B, Perkins ND. A cell cycle regulatory network controlling NFkappaB subunit activity and function. EMBO J 2007; 26:4841-55; PMID:17962807; http://dx.doi.org/10.1038/sj.emboj.7601899
31. Lin HK, Wang G, Chen Z, Teruya-Feldstein J, Liu Y, Chan CH, Yang WL, Erdjument-Bromage H, Nakayama KI, Nimer S, et al. Phosphorylation-dependent regulation of cytosolic localization and oncogenic function of Skp2 by Akt/PKB. Nat Cell Biol 2009; 11:420-32; PMID:19270694; http://dx.doi.org/10.1038/ncb1849
32. Wei W, Ayad NG, Wan Y, Zhang GJ, Kirschner MW, Kaelin WG Jr. Degradation of the SCF component Skp2 in cell-cycle phase G1 by the anaphase-promoting complex. Nature 2004; 428:194-8; PMID:15014503; http://dx.doi.org/10.1038/nature02381
33. Bashir T, Dorrello NV, Amador V, Guardavaccaro D, Pagano M. Control of the SCF(Skp2-Cks1) ubiquitin ligase by the APC/C(Cdh1) ubiquitin ligase. Nature 2004; 428:190-3; PMID:15014502; http://dx.doi.org/10.1038/nature02330
34. Nicholson KM, Anderson NG. The protein kinase B/Akt signalling pathway in human malignancy. Cell Signal 2002; 14:381-95; PMID:11882383; http://dx.doi.org/10.1016/S0898-6568(01)00271-6
35. Santi SA, Lee H. Ablation of Akt2 induces autophagy through cell cycle arrest, the downregulation of p70S6K, and the deregulation of mitochondria in MDA-MB231 cells. PLoS One 2011; 6:e14614; PMID:21297943; http://dx.doi.org/10.1371/journal.pone.0014614
36. Lindsley CW, Zhao Z, Leister WH, Robinson RG, Barnett SF, Defeo-Jones D, Jones RE, Hartman GD, Huff JR, Huber HE, et al. Allosteric Akt (PKB) inhibitors: discovery and SAR of isozyme selective inhibitors. Bioorg Med Chem Lett 2005; 15:761-4; PMID:15664853; http://dx.doi.org/10.1016/j.bmcl.2004.11.011
37. Saxena S, Dutta A. Geminin-Cdt1 balance is critical for genetic stability. Mutat Res 2005; 569:111-21; PMID:15603756; http://dx.doi.org/10.1016/j.mrfmmm.2004.05.026
38. Verdun RE, Crabbe L, Haggblom C, Karlseder J. Functional human telomeres are recognized as DNA damage in G2 of the cell cycle. Mol Cell 2005; 20:551-61; PMID:16307919; http://dx.doi.org/10.1016/j.molcel.2005.09.024
39. Wu Y, Xiao S, Zhu XD. MRE11-RAD50-NBS1 and ATM function as co-mediators of TRF1 in telomere length control. Nat Struct Mol Biol 2007; 14:832-40; PMID:17694070; http://dx.doi.org/10.1038/nsmb1286
40. O'Sullivan RJ, Karlseder J. Telomeres: protecting chromosomes against genome instability. Nat Rev Mol Cell Biol 2010; 11:171-81; PMID:20125188

41. Fraser M, Harding SM, Zhao H, Coackley C, Durocher D, Bristow RG. MRE11 promotes AKT phosphorylation in direct response to DNA double-strand breaks. Cell Cycle 2011; 10:2218-32; PMID:21623170; http://dx.doi.org/10.4161/cc.10.13.16305
42. Bashir T, Pagan JK, Busino L, Pagano M. Phosphorylation of Ser72 is dispensable for Skp2 assembly into an active SCF ubiquitin ligase and its subcellular localization. Cell Cycle 2010; 9:971-4; PMID:20160477; http://dx.doi.org/10.4161/cc.9.5.10914
43. Boutonnet C, Tanguay PL, Julien C, Rodier G, Coulombe P, Meloche S. Phosphorylation of Ser72 does not regulate the ubiquitin ligase activity and subcellular localization of Skp2. Cell Cycle 2010; 9:975-9; PMID:20160482; http://dx.doi.org/10.4161/cc.9.5.10915
44. Wang H, Cui J, Bauzon F, Zhu L. A comparison between Skp2 and FOXO1 for their cytoplasmic localization by Akt1. Cell Cycle 2010; 9:1021-2; PMID:20160512; http://dx.doi.org/10.4161/cc.9.5.10916
45. Chu IM, Hengst L, Slingerland JM. The Cdk inhibitor p27 in human cancer: prognostic potential and relevance to anticancer therapy. Nat Rev Cancer 2008; 8:253-67; PMID:18354415; http://dx.doi.org/10.1038/nrc2347
46. Starostina NG, Kipreos ET. Multiple degradation pathways regulate versatile CIP/KIP CDK inhibitors. Trends Cell Biol 2012; 22:33-41; PMID:22154077; http://dx.doi.org/10.1016/j.tcb.2011.10.004

OPEN ACCESS Freely available online

PLOS ONE

Antitumor Activity and Induction of TP53-Dependent Apoptosis toward Ovarian Clear Cell Adenocarcinoma by the Dual PI3K/mTOR Inhibitor DS-7423

Tomoko Kashiyama[1], Katsutoshi Oda[1]*, Yuji Ikeda[1], Yoshinobu Shiose[2], Yasuhide Hirota[2], Kanako Inaba[1], Chinami Makii[1], Reiko Kurikawa[1], Aki Miyasaka[1], Takahiro Koso[1], Tomohiko Fukuda[1], Michihiro Tanikawa[1], Keiko Shoji[1], Kenbun Sone[1], Takahide Arimoto[1], Osamu Wada-Hiraike[1], Kei Kawana[1], Shunsuke Nakagawa[3], Koichi Matsuda[4], Frank McCormick[5], Hiroyuki Aburatani[6], Tetsu Yano[7], Yutaka Osuga[1], Tomoyuki Fujii[1]

1 Department of Obstetrics and Gynecology, Faculty of Medicine, The University of Tokyo, Tokyo, Japan, **2** Oncology Research Laboratories, Daiichi Sankyo Co. Ltd., Tokyo, Japan, **3** Department of Obstetrics and Gynecology, Faculty of Medicine, Teikyo University, Tokyo, Japan, **4** Laboratory of Molecular Medicine, Human Genome Center, Institute of Medical Science, The University of Tokyo, Tokyo, Japan, **5** Helen Diller Family Comprehensive Cancer Center, University of California San Francisco, San Francisco, California, United States of America, **6** Genome Science Division, Research Center for Advanced Science and Technology, The University of Tokyo, Tokyo, Japan, **7** Department of Obstetrics and Gynecology, National Center for Global Health and Medicine, Tokyo, Japan

Abstract

DS-7423, a novel, small-molecule dual inhibitor of phosphatidylinositol-3-kinase (PI3K) and mammalian target of rapamycin (mTOR), is currently in phase I clinical trials for solid tumors. Although DS-7423 potently inhibits PI3Kα (IC_{50} = 15.6 nM) and mTOR (IC_{50} = 34.9 nM), it also inhibits other isoforms of class I PI3K (IC_{50} values: PI3Kβ = 1,143 nM; PI3Kγ = 249 nM; PI3Kδ = 262 nM). The PI3K/mTOR pathway is frequently activated in ovarian clear cell adenocarcinomas (OCCA) through various mutations that activate PI3K-AKT signaling. Here, we describe the anti-tumor effect of DS-7423 on a panel of nine OCCA cell lines. IC_{50} values for DS-7423 were <75 nM in all the lines, regardless of the mutational status of *PIK3CA*. In mouse xenograft models, DS-7423 suppressed the tumor growth of OCCA in a dose-dependent manner. Flow cytometry analysis revealed a decrease in S-phase cell populations in all the cell lines and an increase in sub-G1 cell populations following treatment with DS-7423 in six of the nine OCCA cell lines tested. DS-7423-mediated apoptosis was induced more effectively in the six cell lines without *TP53* mutations than in the three cell lines with *TP53* mutations. Concomitantly with the decreased phosphorylation level of MDM2 (mouse double minute 2 homolog), the level of phosphorylation of TP53 at Ser46 was increased by DS-7423 in the six cell lines with wild-type *TP53*, with induction of genes that mediate TP53-dependent apoptosis, including *p53AIP1* and *PUMA* at 39 nM or higher doses. Our data suggest that the dual PI3K/mTOR inhibitor DS-7423 may constitute a promising molecular targeted therapy for OCCA, and that its antitumor effect might be partly obtained by induction of TP53-dependent apoptosis in *TP53* wild-type OCCAs.

Citation: Kashiyama T, Oda K, Ikeda Y, Shiose Y, Hirota Y, et al. (2014) Antitumor Activity and Induction of TP53-Dependent Apoptosis toward Ovarian Clear Cell Adenocarcinoma by the Dual PI3K/mTOR Inhibitor DS-7423. PLoS ONE 9(2): e87220. doi:10.1371/journal.pone.0087220

Editor: Yuan-Soon Ho, Taipei Medical University, Taiwan

Received September 30, 2013; **Accepted** December 18, 2013; **Published** February 4, 2014

Funding: This work was supported by Daiichi Sankyo Co. Ltd., The Grant-in-Aid for Scientific Research (C), Grant Number 19599005 and 23592437 from the Ministry of Education, Culture, Sports, Science and Technology of Japan (to K Oda). This study was also performed as a research program of the Project for Development of Innovative Research on Cancer Therapeutics (P-Direct), Ministry of Education, Culture, Sports, Science and Technology of Japan (to T Yano). Yoshinobu Shiose and Yasuhide Hirota, employees of Daiichi Sankyo Co. Ltd, contributed to the experiments (in vivo experiments) as listed in the "contributions" of each author. The funders themselves had no role in study design, data collection and analysis, decision to publish, or preparation of the manuscript.

Competing Interests: Yoshinobu Shiose and Yasuhide Hirota are employees of Daiichi Sankyo Co. Ltd, which partly supported this work (to K Oda). DS-7423 is in clinical development by Daiichi Sankyo Co. Ltd and was provided by the company for use in this study. There are no other relevant COI related to employment, consultancy, patents, products in development, or marketed products. These COI do not alter the authors' adherence to all the PLOS ONE policies on sharing data and materials.

* E-mail: katsutoshi-tky@umin.ac.jp

Introduction

The phosphatidylinositol 3-kinase (PI3K)-AKT signaling pathway is frequently activated in various types of cancers, and several inhibitors that target this pathway have been developed as potential cancer therapeutics. The constitutive activation of the PI3K-AKT pathway results from various types of alterations, including the overexpression of receptor tyrosine kinases (RTKs), as well as mutations of *Ras*, the catalytic subunit p110α of phosphoinositide-3-kinase (*PIK3CA*), and *PTEN* [1]. Class I PI3Ks include four isoforms of the catalytic subunit (p110α, p110β, p110γ, and p110δ). Among these four isoforms, p110α is broadly mutated and predominantly activated in various types of human cancers, although p110β and p110δ might be selectively activated in certain tumors such as those with loss of PTEN function [2,3]. Mammalian target of rapamycin (mTOR) is the catalytic subunit found in two distinct complexes: the raptor-containing complex mTORC1 and the rictor-containing complex mTORC2 [4]. AKT activates mTORC1 signaling and also phosphorylates other downstream proteins, including GSK3β, forkhead box-O tran-

scription factors (FOXOs), and mouse double minute 2 homolog (MDM2) [5]. mTORC1 controls protein synthesis and cell proliferation via the phosphorylation of its downstream targets, 4E-BP1 and S6 kinase 1 (S6K1) [6]. Rapamycin and its analogs (rapalogs) block mTORC1 activity, but not mTORC2 activity [7]. One of the AKT downstream targets, MDM2, is a negative regulator of TP53 that induces its ubiquitination and subsequent degradation [8]. Although the cytostatic effects of PI3K pathway inhibitors have been reported in various types of cancers [9–12], targeting the PI3K pathway might induce cytotoxic effects by suppressing anti-apoptotic signals through the dephosphorylation of FOXOs and stabilization of TP53. It seems reasonable to suspect that targeting the PI3K-mTOR axis might be a promising therapeutic strategy to selectively induce apoptosis of cancer cells, especially those without mutations in *TP53*.

Epithelial ovarian cancer is a leading cause of death resulting from gynecological malignancies. Ovarian clear cell adenocarcinoma (OCCA) is the second most common cause of death from ovarian cancer, with a higher incidence in Asia, especially in Japan (>25%), than in other continents [13]. OCCA is derived primarily from ovarian endometriosis, and the clinical outcome is generally poor, owing to low response rates to conventional platinum-based chemotherapy [14]. Thus, novel therapeutic strategies are warranted to improve the clinical outcome of OCCA. In histological terms, ovarian serous adenocarcinoma (OSA) is the most common variant of ovarian carcinoma [15]. It is highly sensitive to platinum-based chemotherapy, with a primary clinical response rate of >70%. The mutational spectrum differs between OCCA and OSA, with *TP53* mutations observed in almost all (96%) OSA tumors, but in only 10% of OCCA tumors [15,16]. In particular, mutations of *RB1* and *BRCA1/2* are much more common in OSA than in OCCA. However, *PIK3CA* mutations are more frequent in OCCA (>40%) than in OSA (<10%) [17]. Although mutations of *KRAS* and *PTEN* are rare (<10%), the overexpression of several RTKs has been reported in OCCA, including human epidermal growth factor receptor 2 (HER2) with a frequency of approximately 40% and cMET with a frequency of approximately 30% [18–21]. Taken together, these observations suggest that the RTK-PI3K/mTOR signaling axis might be broadly activated in OCCA.

DS-7423 is a novel, small-molecule compound that inhibits both PI3K and mTOR (mTORC1/2). It inhibits all class I PI3K isoforms with greater potency against p110α than against the other p110 isoforms. Relevant activity (IC_{50} <200 nM) was not observed in any of the 227 kinases tested, except for Mixed Lineage Kinase 1 (MLK1) and Never-In-Mitosis Gene A (NIMA)-related kinase 2 (NEK2). The compound is currently in phase I clinical trials for solid tumors. In this study, we evaluated its anti-tumor efficacy in a panel of OCCA cell lines. We focused in particular on the ability of DS-7423 to induce apoptosis, and on whether the apoptosis might be mediated by TP53.

Materials and Methods

Small-molecule compounds

The small molecule compound DS-7423 was provided by the Daiichi-Sankyo Company, Ltd (Tokyo, Japan). The drug information about DS-7423 is available on the ClinicalTrials.gov website (NCT01364844). The mTOR inhibitor rapamycin was purchased from Cayman Chemical (Michigan, USA).

Cell lines

The OVTOKO, OVISE, OVMANA, RMG-I, OVSAHO, OVKATE, and OV1063 lines were purchased from the Japanese Collection of Research Bioresources (JCRB) Cell Bank (Osaka, Japan). The JHOC-7, JHOC-9, HTOA, JHOS-2, JHOS-3, and JHOS-4 cell lines were purchased from the RIKEN Cell Bank (Ibaraki, Japan). The TOV-21, ES-2, and SKOV3 cell lines were from the American Type Culture Collection (Manassas, VA). OVISE, OVTOKO, TOV-21G and ES2 were cultured in RPMI1640 medium containing 10% fetal bovine serum (FBS). OVMANA was cultured in RPMI medium containing 20% FBS, JHOC-7 in DMEM/F12 medium containing 10% FBS, JHOC-9 and RMG-I in DMEM/F12 medium containing 20% FBS, and SKOV3 in DMEM containing 10% FBS. The OVSAHO, OVKATE, OV1063, HTOA, JHOS-2, JHOS-3, and JHOS-4 lines were cultured in DMEM medium containing 10% FBS. The histological subtype of the SKOV3 cells was not unambiguously defined even after extensive analysis, although it was confidently identified as clear cell adenocarcinoma [22]. The immortalized epithelial cell line from an ovarian endometrial cyst was a generous gift from Dr. Satoru Kyo [23].

Polymerase chain reaction (PCR) and sequencing

The mutational status of all nine OCCA cell lines was analyzed by PCR and direct sequencing. The PCR conditions and primers for the analysis of *PTEN* (exons 1–9) and *K-Ras* (exon 1 and 2) sequences were described previously [24–26]. The entire coding region of *PIK3CA* was analyzed by reverse transcription (RT)-PCR with LA-Taq according to the manufacturer's protocol (Takara BIO, Madison, WI) [27]. The PCR primers for analysis of *TP53* (exons 4–8) were described previously [28].

Proliferation assays

Assays of the suppression of cell proliferation were performed with the Cell Counting Kit-8 using the tetrazolium salt WST-8 [2-(2-methoxy-4-nitrophenyl)-3-(4-nitrophenyl)-5-(2,4-disulfophenyl)-2H-tetrazolium, monosodium salt] (Dojindo, Tokyo, Japan) for the methyl thiazolyl tetrazolium (MTT) assay. Using 96-well plates, 2,000 cells were seeded on the appropriate medium and treated with increasing doses (0–2,500 nM) of DS-7423 or rapamycin for 72 h, starting from 24 h after seeding. Proliferation was quantified by monitoring the changes in the absorbance at 450 nm, which were normalized relative to the absorbance of cell cultures treated with DMSO alone.

Immunoblotting

Cells were treated with DS-7423 or rapamycin for the indicated time and at the indicated concentration, and were then lysed in the cell lysis buffer (Cell Signaling Technology, Beverly, MA). Antibodies to total Akt, phosphorylation of Akt (p-Akt) (Ser473, Thr308), p-GSK3beta (Ser9), total S6, p-S6 (Ser235/236, Ser 240/244), p-4EBP1 (Thr37/46), p-FOXO1 (Thr24), p-FOXO3a (Thr32), p-MDM2 (Ser 166), p-TP53 (Ser15), cleaved-PARP, and PARP (Cell Signaling Technology, Beverly, MA), beta-actin (Sigma-Aldrich, St. Louis, MO), TP53 (Santa Cruz, CA, USA) and p-TP53 (Ser46) (Calbiochem, Billerica, MA) were used for immunoblotting, as recommended by the manufacturers. Signals were detected using BioRAD western blotting systems (BioRAD, Hercules, CA) with the detection reagents ECL advance and ECL select (GE Healthcare, Piscataway, NJ).

Cell cycle analysis

Cells (5×10^5) were seeded in 60-mm dishes and treated with DS-7423 for 48 h. Floating and adherent cells were collected by trypsinization and washed twice with phosphate buffer saline (PBS). Cells were resuspended in cold 70% ethanol and

maintained at 4°C overnight. After being washed twice with PBS, cells were incubated in RNase A (0.25 mg/mL) (Sigma) for 30 min at 37°C, followed by staining with propidium iodide (PI; 50 μg/mL) (Sigma) at 4°C for 30 min in the dark. Cells were then analyzed using flow cytometry (BD FACS Calibur HG, Franklin Lakes, NJ). Cell cycle distribution was analyzed using CELL Quest pro ver. 3.1. (Beckman Coulter Epics XL, Brea, CA). All experiments were repeated three times.

Detection of apoptosis by staining with annexin-V FITC

Cells (5×10^5) were cultured in 60-mm plates for 24 h before treatment with either DMSO (control), and 156 nM DS-7423, or 2,500 nM DS-7423 for 48 h. Cells were trypsinized, washed twice with PBS, and then analyzed after double staining with annexin-V fluorescein isothiocyanate (FITC) (Abcam, Cambridge, MA) and PI. The apoptotic cell population was analyzed using flow cytometry. All experiments were performed three times.

Ethics statement for animal experiments

This study was approved by Animal Care and Use Committee, Daiichi-Sankyo Pharmaceutical Co. Ltd. Athymic mice were maintained in an SPF (Specific Pathogen Free) facility according to our institutional guidelines, and experiments were conducted under an approved animal protocol.

Tumor xenografts in nude mice

Specific pathogen-free female nude mice (BALB/cAJcl-nu/nu), 6 weeks old, were purchased from CLEA Japan, Inc (Tokyo, Japan). Subcutaneous xenograft tumors in the mice were established by the injection of a 100-μL suspension containing 5×10^6 cells of the TOV-21, RMG-I, or ES-2 lines in PBS. Tumors were removed after exponential growth, cut into 3-mm pieces, and transplanted subcutaneously into other mice for RMG-I cells. DS-7423 was suspended in 0.5 w/v% Methyl Cellulose 400 solution (Wako Pure Chemical Industries, Ltd.) Oral daily administration of DS-7423 started 8–22 days later, following the injection of the cells ($5–6\times10^6$ cells/0.1 mL). One week after tumor transplantation, mice were assigned randomly to one of the three treatment regimens: (1) non-treated control, (2) DS-7423 (1.5 mg/kg), (3) DS-7423 (3 mg/kg), and (4) DS-7423 (6 mg/kg). Each treatment group consisted of five mice. DS-7423 was injected orally (p.o.) once a day. Tumor volumes (in mm^3) were calculated by the formula: ([major axis] × [minor axis]^2/2). After the treatment, the tumors were removed and analyzed by western blotting. Tumor weight (wet weight) was measured, and the average weight was calculated for each group.

Semi-quantitative RT-PCR analysis

OCCA cells were treated with either DMSO or the indicated concentration of either DS-7423 or rapamycin for 24 h. Total RNAs of these cells were extracted with the RNeasy Mini Kit according to the manufacturer's instructions (QIAGEN, Valencia, CA). cDNAs were synthesized from total RNAs by using the Super Script III First-strand Synthesis SuperMix (Invitrogen, Carlsbad, CA). The exponential phase of the RT-PCR occurred between 15–30 cycles, and these cycles were monitored to allow semi-quantitative comparisons among the cDNAs developed from identical reactions. The primers and conditions for the amplification of *p53AIP1*, *p21*, and *GAPDH* sequences were described previously [29]. The PCR primers for *PUMA* were 5′-TGAGACAAGAGGAGCAGCAG-3′ (forward) and 5′-ACCTAATTGGGCTCCAT CTC-3′ (reverse). The primers for p53R2, TIGAR, GLS2, GADD45, 14-3-3 sigma and PAI-1 were described previously [30–35]. Each PCR regimen involved a 2-min initial denaturation step (94°C), which was followed by 15–30 cycles at 94°C for 30 s, then at 55°C for 30 s, and finally, at 72°C for 30 s using a Thermal Cycler Gene Atlas instrument (ASTEC, Fukuoka, Japan).

Gene silencing

Cells were plated at approximately 30% confluence in 100-mm plates and incubated for 24 h before transfection with small interfering RNA (siRNA) duplexes at the concentrations indicated, using Lipofectamine 2000 RNAiMAX (Invitrogen, Carlsbad, CA) and Opti-MEM medium (Life Technologies, Grand Island, NY). The siRNAs specific for TP53 were purchased from Invitrogen. A negative control kit was used as a control (Invitrogen, Carlsbad, CA).

Luciferase assay

Transfection was performed using Effectene reagent (QIAGEN, Valencia, CA) according to the manufacturer's recommendation. The TP53 expression plasmid (0.1 μg/μL) was cotransfected with pp53 TA Luc (0.25 μg/mL). The phRL CMV-Renilla plasmid (Promega, Madison, WI) was also transfected in all experiments as the internal control to normalize the transfection efficiency. The assays, each involving triplicate wells, were repeated three times.

Statistical analysis

The data were expressed as means ± standard deviations of three independent determinations. The significance of the difference between two samples was analyzed using the Student's t-test, and a p-value of <0.05 was considered to denote a statistically significant difference.

Results

Genetic alterations and activation of the PI3K-AKT signaling pathway in OCCA cell lines

We evaluated the phosphorylation (p-) levels of the proteins in the PI3K-AKT pathway by using an immortalized epithelial cell line from an ovarian endometrial cyst as a control. AKT was phosphorylated at Thr308 in seven of the nine OCCA cell lines tested (Figure 1). The cell lines OVMANA and ES-2 had low levels of p-AKT (Thr308) (Figure 1). The phosphorylation levels of S6, 4E-BP1 and/or FOXO1/3a, the downstream targets of AKT, were upregulated in the OCCA cells, including OVMANA and ES-2.

Four of the nine cell lines possessed *PIK3CA* mutations (44%) (Figure 1 and Table S1), and one of these four, TOV-21G, also possessed mutations in *PTEN* and *K-Ras* (11%). *TP53* mutations were detected in three cell lines (33%) (Table S1). The mutational status of *PIK3CA* was not associated with the phosphorylation of AKT or proteins that act downstream of AKT. Next, the expression and phosphorylation levels of three RTKs (HER2, HER3, and MET), which have been reported to be overexpressed in OCCA, were evaluated. The levels of phosphorylation of both HER2 (Tyr1221/1222) and HER3 (Tyr1289) were correlated with the abundances of these two proteins (Figure 1). p-HER2 and p-HER3 levels were elevated in four (44%: OVISE, SKOV3, JHOC7 and RMG-I) and six (67%: TOV-21G, OVISE, OVMANA, OVTOKO, JHOC-7 and RMG-I) cell lines, respectively (Figure 1). The expression of MET was higher in all nine OCCA cell lines than in the control, although the level of p-MET was increased in only two cell lines (22%: JHOC-7 and RMG-I). Taken together, all the OCCA cell lines, except for ES-2 and JHOC-9, possessed one or more activating alterations in the RTK-PI3K genes examined (Figure 1 and Table S1). Each of the

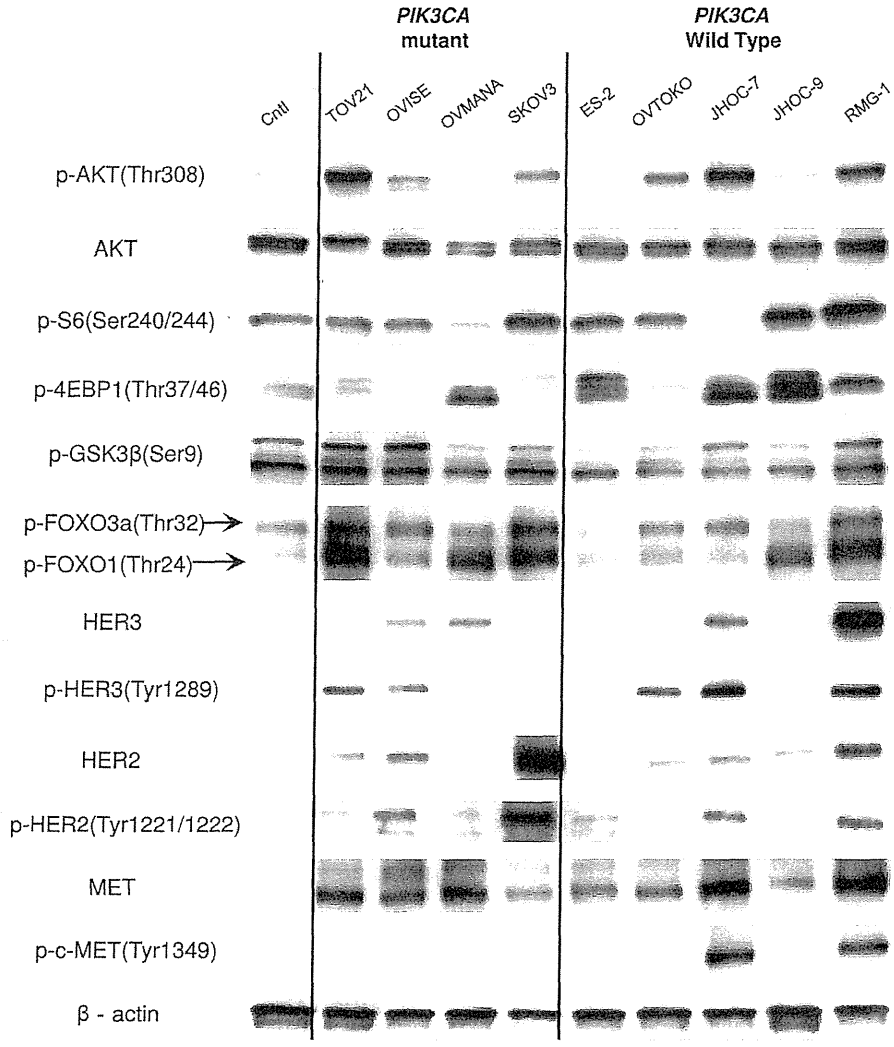

Figure 1. Phosphorylation and mutational status of genes that encode components of the RTK/Ras/PI3K pathway. Nine ovarian clear cell adenocarcinoma (OCCA) and a control (Cntl) cell line (immortalized epithelial cells from ovarian endometrioma) were lysed in cell lysis buffer and analyzed by western blotting. In general, most of the OCCA cell lines displayed higher levels of phosphorylation of Akt (Thr308) and its downstream targets (GSK3β, FOXO 1/3a, 4EBP1 and S6) than the respective levels of phosphorylation in the control line. The abundances and levels of phosphorylation of c-MET (Tyr1234/1235), HER2 (Tyr1221/1222), and HER3 (Tyr1289) were also evaluated. The mutational status of *PIK3CA*, *PTEN*, and *K-Ras* is shown for each cell line.
doi:10.1371/journal.pone.0087220.g001

four cell lines with *PIK3CA* mutations showed concomitant activation of RTKs, defined as high levels of phosphorylation of HER2 and/or HER3.

Anti-proliferative effect of DS-7423 in OCCA cell lines

We tested the anti-proliferative effects of the dual PI3K/mTOR inhibitor, DS-7423, and the mTOR (mTORC1) inhibitor, rapamycin, in each of the nine OCCA cell lines. Exposure to 156 nM DS-7423 inhibited cell growth by 70%–97%, and the IC_{50} values for cell proliferation were 20–75 nM (Figure 2A). Dose-dependent growth suppression was more clearly induced by DS-7423 than by rapamycin in each of the nine cell lines (Figure 2A). The IC_{50} value was not reached with rapamycin at any of the concentrations tested (2.45–2,560 nM) in five (OVMANA, SKOV3, OVTOKO, JHOC-7 and RMG-I) of the nine OCCA cell lines. We also examined the effect of DS-7423 in seven OSA lines. The IC_{50} values with DS-7423 were >100 nM in four of these seven OSAs (Figure 2B). The ratio of resistant cell lines (IC_{50} >100 nM) was significantly higher in OSA cell lines (57%) than in OCCA cell lines (0%) ($p = 0.019$ by Fisher's exact test).

We performed immunoblotting on the lysates prepared from the cells treated with DS-7423 or rapamycin. DS-7423 suppressed the phosphorylation of AKT (Thr308 and Ser473) and S6 (Ser235/236 and Ser240/244) at doses of 39–156 nM and higher (Figure 3A and Figure S1). DS-7423 suppressed the phosphorylation levels of the targeted proteins at comparable doses in the AKT pathway (AKT, FOXO1/3a, and MDM2) and mTORC1 pathway (S6). Rapamycin did not suppress p-Akt at any dose, and suppressed p-S6 at 2.45 nM or higher doses (Figure 3B). On the

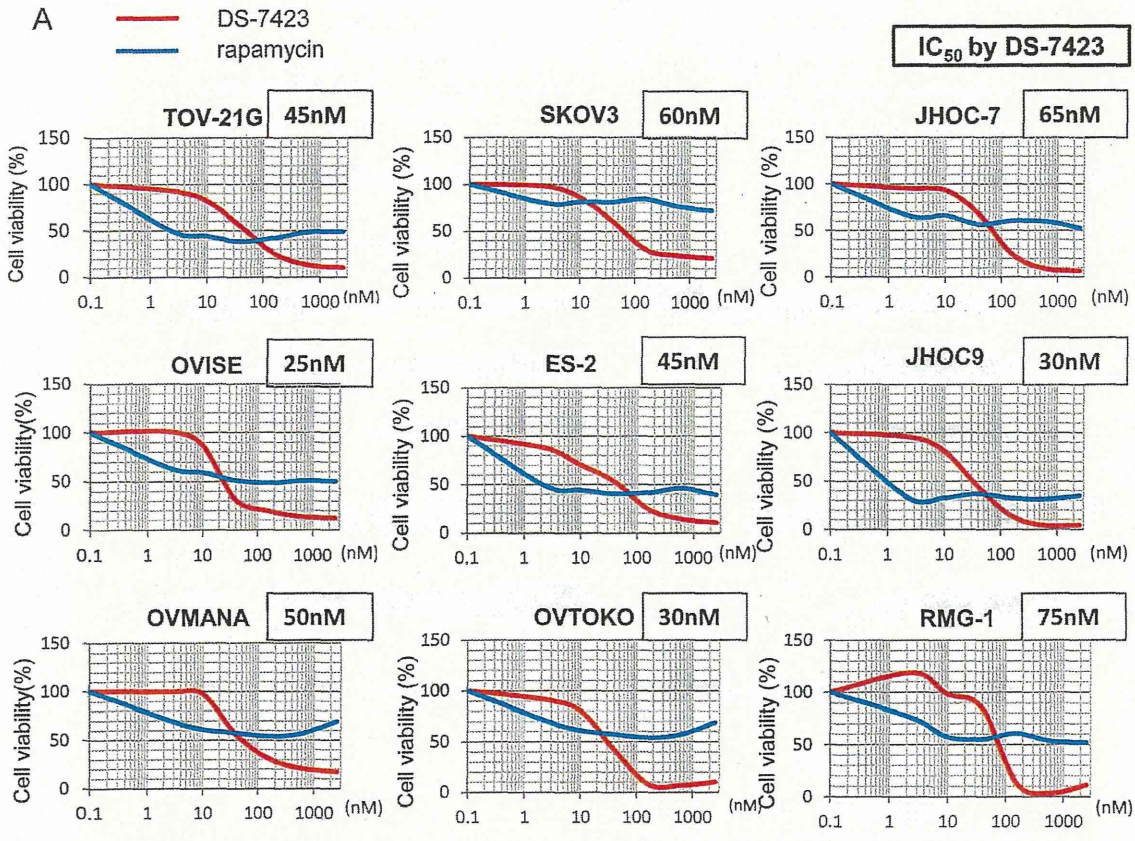

B

OSA	IC_{50} (nM)
JHOS-3	45
HTOA	60
OVSAHO	65
JHOS-4	120
JHOS-2	250
OV1063	700
OVKATE	>2,500

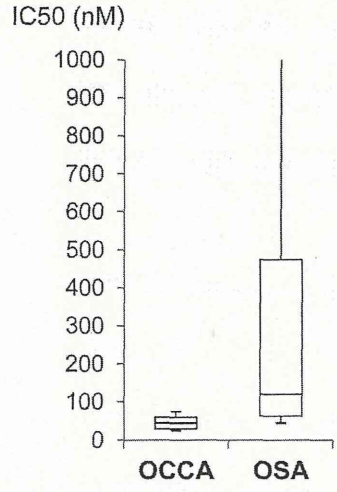

Figure 2. Inhibition of cell proliferation by DS-7423 and rapamycin. (A) Cell viability for each cell line was analyzed using the methyl thiazolyl tetrazolium (MTT) assay 72 h after treatment with DS-7423 or rapamycin at the doses indicated. The data were normalized relative to the value of the control cells. In all nine cell lines, DS-7423 suppressed cell proliferation more robustly than rapamycin when both were used at higher doses. (B) IC_{50} values for DS-7423 in seven ovarian serous adenocarcinoma (OSA) cell lines (left) were compared with those of nine OCCA cells (right). Four of seven OSA cells had IC_{50} values >100 nM, which is higher than that of any OCCA cells.
doi:10.1371/journal.pone.0087220.g002

contrary, rapamycin increased the levels of p-FOXO3a and p-FOXO1 at 2,500 nM (Figure 3B).

We conducted fluorescence-activated cell sorting (FACS)-based cell cycle analyses in OCCA cells treated with DS-7423. DS-7423 decreased the size of the S-phase population in the

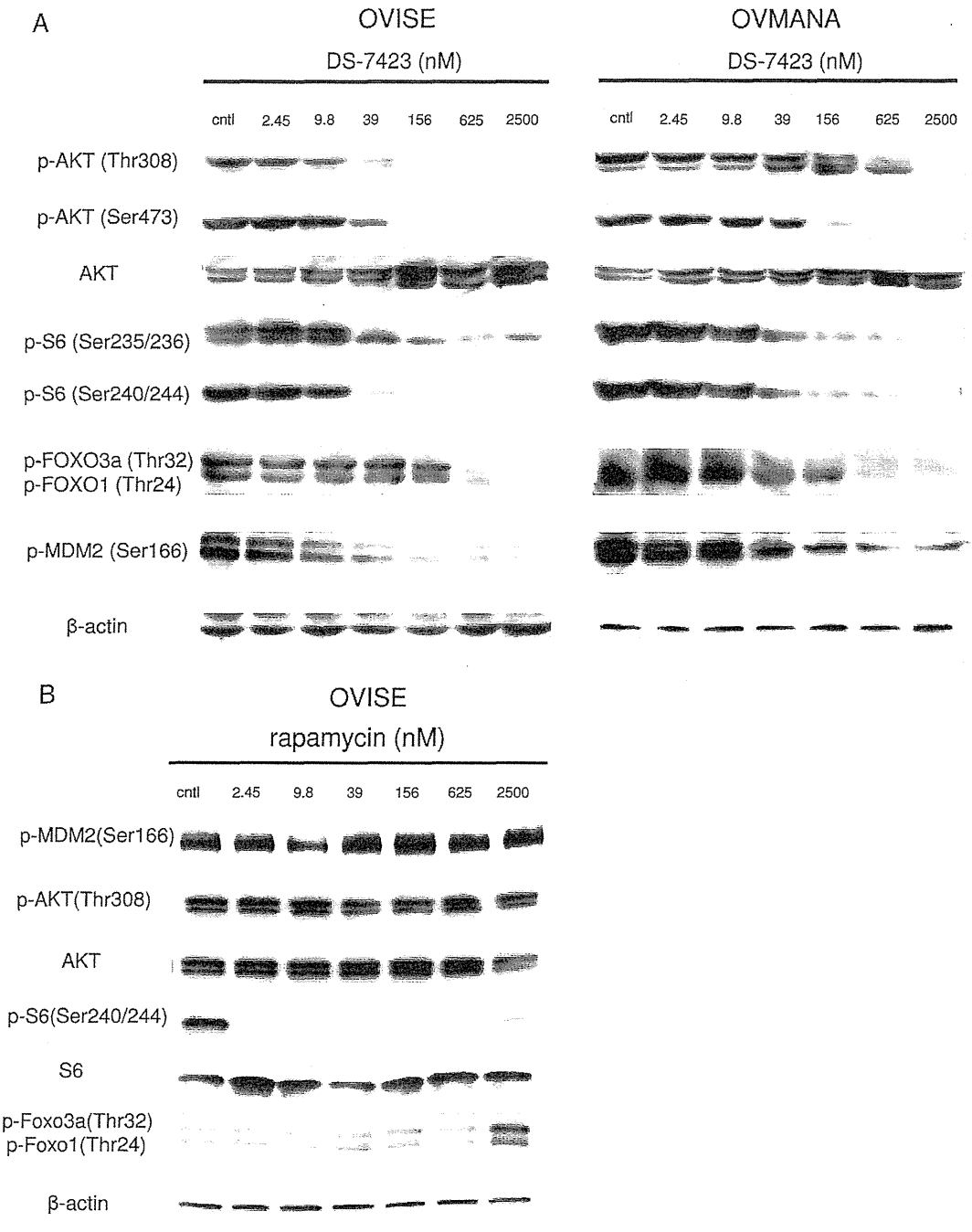

Figure 3. Inhibition of PI3K/mTOR signaling by DS-7423 and rapamycin in ovarian clear cell adenocarcinoma cell lines. (A) Immunoblotting of total protein extracts from OCCA cells (OVISE and OVMANA) treated with DS-7423 at concentrations ranging from 0 to 2,500 nM. (B) Immunoblotting of total protein extracts from OVISE cells treated with rapamycin at concentrations ranging from 0 to 2,500 nM.
doi:10.1371/journal.pone.0087220.g003

OCCA cells, although the change was weak in ES-2 cells. (Figure 4A). G1 arrest was predominantly observed in six of the nine cell lines. The sizes of sub-G1 populations increased in a dose-dependent manner in six of the nine cell lines, especially in OVISE and OVMANA cells.

In vivo antitumor effect of DS-7423 in a mouse xenograft model

In vivo antitumor activity of DS-7423 in mice implanted with either TOV-21G cells or RMG-1 tumor pieces was examined. Oral daily administration of DS-7423 significantly suppressed the tumor growth of the xenografts of TOV-21G and RMG-I in a

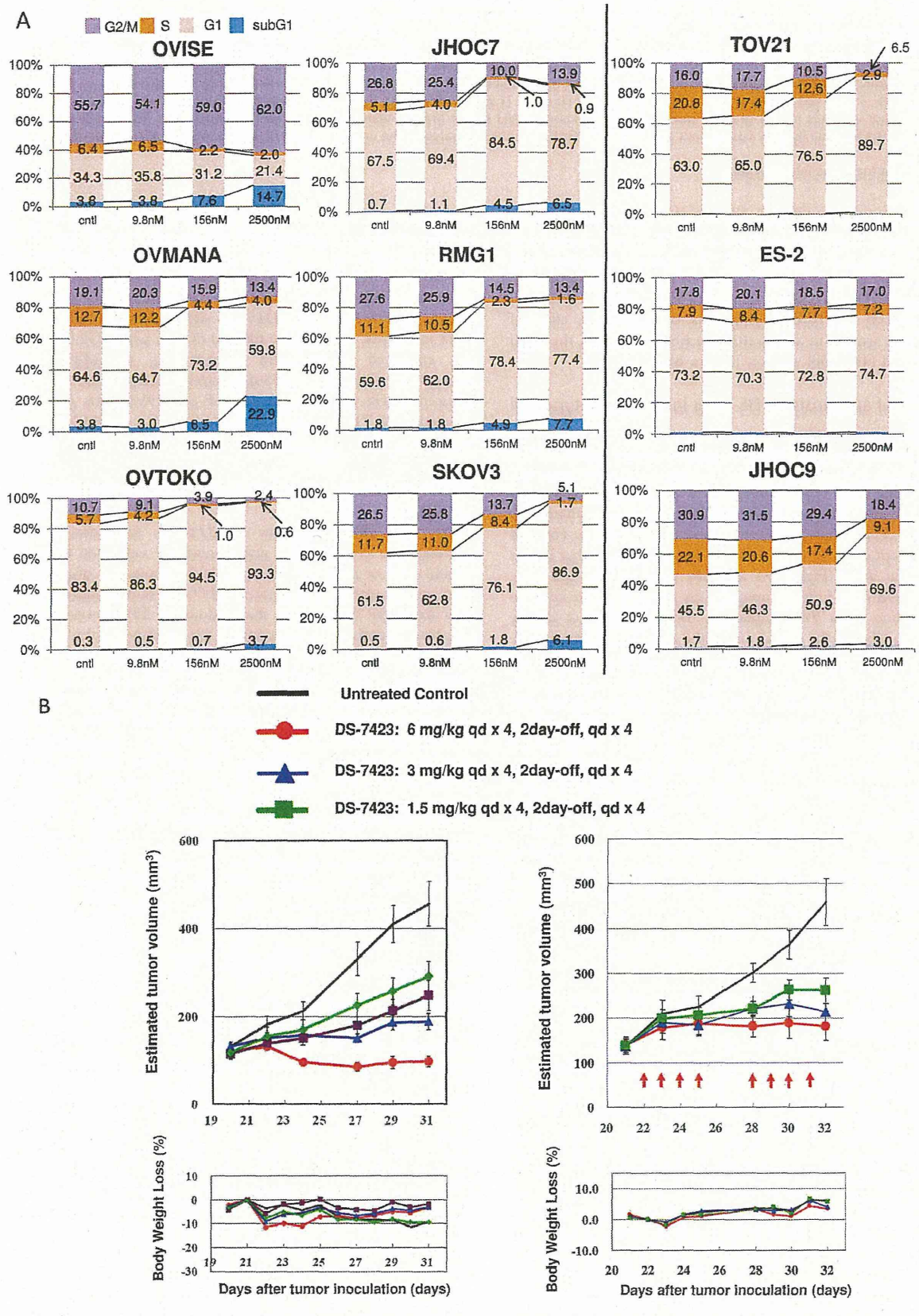
A
G2/M
S
G1
subG1
OVISE
JHOC7
TOV21
OVMANA
RMG1
ES-2
OVTOKO
SKOV3
JHOC9
cntl
9.8nM
156nM
2500nM
cntrl
B
Untreated Control
DS-7423: 6 mg/kg qd x 4, 2day-off, qd x 4
DS-7423: 3 mg/kg qd x 4, 2day-off, qd x 4
DS-7423: 1.5 mg/kg qd x 4, 2day-off, qd x 4
Estimated tumor volume (mm3)
Body Weight Loss (%)
Days after tumor inoculation (days)

Figure 4. Flow cytometric analysis of the cell cycle in cancer cells treated with DS-7423, and *in vivo* demonstration of the anti-tumor effect of DS-7423 in nude mice. (A) Cells (5×10^5) were seeded in the presence of 10% serum and treated with DS-7423 for 48 h at doses of 9.8 nM, 256 nM, or 2,500 nM. DS-7423 blocked OCCA cell cycle progression into the S phase in a dose-dependent manner. The relative size of the sub-G1 population was increased in six of the cell lines (left) but was not affected in the remaining three cell lines (right). (B) Subcutaneous xenograft tumors in athymic BALB/c mice were established following the injection of OCCA cells of either the TOV-21G (left) or RMG-I (right) cell lines. Mice were treated daily (5–7 days per week) at the indicated doses of DS-7423 (1.5, 3, or 6 mg/kg, 8–10 days). Each treatment group contained five mice. Estimated tumor volumes (upper graphs) and body weight losses (BWL) (lower graphs) were shown in the two OCCA cells. Tumor volumes were calculated by the formula {(major axis)*(minor axis)^2/2} mm^3. Groups were compared at the end of treatment. Points, mean; bars, standard deviation (SD); *$p<0.05$.
doi:10.1371/journal.pone.0087220.g004

dose-dependent manner (Figure 4B). No significant adverse effects, including body weight loss of more than 10%, were observed in the mice examined (Figure 4B). Treatment with DS-7423 suppressed the levels of p-AKT (Thr308) and p-S6 (Ser240/244) in the TOV-21G and RMG-I xenografts (Figure S2A). Compared with TOV-21G and RMG-I xenografts, the anti-tumor effect of DS-7423 was weaker in xenografts with ES-2, for which the basal level of p-Akt (Thr-308) was low (Figure S2B).

Induction of apoptosis by DS-7423 in TP53 wild-type cell lines

The data collected from FACS analysis suggested that DS-7423 has a cytotoxic and cytostatic effect in certain OCCA cell lines. We combined the DS-7423 treatment (156 nM or 2,500 nM) with double staining with annexin-V FITC and PI to evaluate the proportion of cells that underwent apoptosis. DS-7423 at 156 nM induced apoptosis at 4–12% in five of the six cell lines that lacked mutations in *TP53* (Figure 5A and 5B). In these five cell lines, 2,500 nM DS-7423 induced apoptosis in 10–16% of the cells. In three cell lines with *TP53* mutations, DS-7423 did not induce apoptosis in >5% of the cells at any of the doses tested (Figure 5A). The size of the population of apoptotic cells was significantly higher in cells that lacked mutations in *TP3* when compared with cells with mutated *TP3* at either 156 nM ($p = 0.0352$) or 2,500 nM ($p = 0.0368$) DS-7423 according to the Student *t*-test (Figure 5C). Rapamycin did not induce apoptotic cell death in >5% of the OCCA cells, even at 2,500 nM. The percentage of apoptotic cells was significantly higher in OVISE cells treated with DS-7423 than that in those treated with rapamycin (Figure S3). This result indicates that mTORC1 inhibition alone is insufficient to induce apoptosis in OCCA cell lines. Immunoblotting analysis revealed that DS-7423 induced the cleavage of PARP within 2 h in OVMANA cells without mutations in *TP53* (Figure 5D). The induction of cleaved-PARP was observed at 39 nM, and the effect increased in a dose-dependent manner up to a concentration of 2,500 nM (Figure 5D).

Induction of p-TP53 at Ser46 and expression of *p53AIP1* by DS-7423

The phosphorylation of MDM2 is associated with the activation of MDM2 and degradation of TP53, with the phosphorylation of TP53 at Ser46 playing a key event in the TP53-dependent apoptosis (28). Treatment with DS-7423 reduced the level of p-MDM2 in a dose-dependent manner (Figure 3A and 6A). Inversely, DS-7423 increased TP53 level even at lower doses, resulting in increased expression of p-TP53 (Ser15 and Ser46) (Figure 6A). However, only p-TP53 (Ser46), not p-TP53 (Ser15), was clearly induced by high doses of DS-7423 (156–2,500 nM). We then used semi-quantitative RT-PCR to evaluate the regulation of genes that are directly regulated by TP53 in OVMANA and OVISE cells. DS-7423 induced the expression of the pro-apoptotic genes *p53AIP1* and *PUMA* at 39 nM or higher doses, but did not induce the expression of p21 at any of the three doses tested (39, 156, and 2,500 nM) (Figure. 6B and 6C). We also performed semi-quantitative RT-PCR of other TP53 target genes involved in DNA repair (p53R2), metabolism (TIGAR and GLS2), G2/M arrest (GADD45), and cell cycle arrest/senescence (14-3-3 sigma and PAI-1) to test whether other TP53 target genes are induced by DS-7423. GADD45 was significantly induced by DS-7423 in OVISE cells (Figure 6B and 6C), in which G2/M arrest was enhanced by DS-7423 according to the MTT assay (Figure 4A). The other TP53-downstream genes tested were not induced by DS-7423 in both OVISE and OVMANA cells, and expression of TIGAR was rather decreased in OVMANA cells (Figure S4).

TP53 activation is responsible for DS-7423-mediated apoptosis

We used siRNAs specific to *TP53* to knockdown *TP53* expression in OVISE cells, and treated the cells with DS-7423 at either 156 or 2,500 nM. The size of the population of apoptotic cells was calculated by annexin-V FITC–PI double staining 48 h after treatment of DS-7423. Knockdown of TP53 levels rescued cells from apoptotic cell death induced by treatment with both DS-7423 doses (Figure 6D). Immunoblotting indicated that two independent siRNAs (siRNA1 and siRNA2) specific to TP53 suppressed the expression of TP53 by >80% (Figure 6E). Next, we performed the MTT assay by applying both DS-7423 and siRNA to TP53 in OVISE cells (wild-type TP53). The anti-proliferative effect of DS-7423 was significantly reduced when combined with the knockdown of TP53 (Figure 6F). The effect of DS-7423 on the transcriptional activity of TP53 was also examined by luciferase assays in ES-2 cells with mutations in *TP53*. The cells were treated with DS-7423 for 24 h at the indicated doses, and then cotransfected with both pp53-TA-luc plasmid (containing TP53 binding sites) and a plasmid that encodes TP53. The relative luciferase activity of TP53 was significantly enhanced by DS-7423 in a dose-dependent manner (Figure 6G).

Discussion

The effects of the PI3K/mTOR inhibitor, DS-7423, on OCCA cell lines were examined with a particular focus on (i) the anti-proliferative effect of DS-7423, (ii) the induction of apoptosis by DS-7423, and (iii) the identification of predictive biomarkers for (i) and (ii).

MTT assays revealed a clear dose-dependent effect of DS-7423 on cell proliferation, with all nine OCCA cell lines displaying sensitivity to DS-7423 (IC_{50} at 75 nM or lower), regardless of mutations on *PIK3CA*. The sensitivity to DS-7423 was significantly higher in OCCA than in OSA cell lines. The prevalence in OCCA cell lines of activating mutations in genes that encode components of the RTK-PI3K-AKT signaling pathway might account, at least in part, for their broad sensitivity to DS-7423. Differences in the dose-dependence of the anti-proliferative effects of DS-7423 and rapamycin suggest differences in the modes of action of these two drugs. Whereas DS-7423 showed a more robust anti-proliferative